PROGRESSIVE ALBITISATION IN THE "MIGMATITE CREEK" REGION, WEEKEROO INLIER, CURNAMONA

Thesis submitted for the degree of
Master of Science
Geology &Geophysics
School of Earth & Environmental Sciences
The University of Adelaide

by

CHENG LIN YANG

July 2008

3 RESULTS

3.1 Mapping of Migmatite Creek

The mapping of the Migmatite Creek area was carried out at a scale of 1:10,000 supported by ArcGIS. The incentive was to compile a thematic map of the albitised units of approximately 3 km^2 of the Migmatite Creek area (Figure3.1). The map is accompanied by 53 photos and 41 samples from outcrops and rock types to illustrate the appearance of variable types and degrees of albitisation in the field. The geological boundaries were mapped along three crosscutting sections and along the lithological boundaries in and adjacent to the area. The following geological boundaries were mapped (Chapter 1.5.1):

1) between the evolving Adelaidean conglomerate and the basement (unconformity),
2) between the migmatite unit (FEM) and the albitisation unit (Plf),
3) between metasediments and specific units e.g. amphibolite, quartz veins and pegmatites.
4) intensity of albitisation using an arbitrary scale of:
    a. high intensity albitisation,
    b. medium intensity albitisation
    c. low intensity albitisation.

All boundaries and sampling were located by using GPS data. The albitisation units were closely related to the fold axes/hinges, the breccias, biotite alteration and areas of evident migmatization.

3.1.1 Albitisation Units

Mapping of albitisation gradients is across and along stratigraphic boundaries. Albitisation units cover different lithologies in the geochemical map.

To the east the mapped Palaeoproterozoic units of the Willyama Supergroup are unconformably overlain by the basal conglomerate of the Adelaidean system (the base of the Burra Group). The dominating lithology in the mapping area is the Migmatite unit (FEM) in both the southern and northern parts of the area (Figure 3.2). In the northwestern section of the area the FEM comprises migmatitic retrograde-gneisses and metasediments with distinct organic components intruded by pegmatites. In the southeastern section of the area the FEM contains at least 4 types of large pegmatite bodies. The differences reflect both, the compositional variability of the original rock and the metamorphic and metasomatic overprint with a decreasing degree of migmatisation from the southeast to northwest. The base of the Plf unit does not outcrop evenly in the centre of antiformal hinges of the Migmatite Creek antiform.

The Plf unit is present throughout the mapped area. The unit is subdivided into seven sub-units based on the intensities of albitisation as observed in the field. The seven units are:

- high-intensity albitisation zones (HA),
- medium-intensity albitisation zones (MA),
- low-intensity albitisation zones (LA),
- amphibolite,
- pegmatite,
- quartz veins and
- breccias.

The High – Medium - Low albitisation units were classified by visual estimate of albite content. Their mineral assemblages are albite + quartz + magnetite/hematite + micas ± accessory minerals.

The high intensity albitisation unit (HA) is white to light grey and contains breccia pipes and fracture networks striking in about 60 degree including two groups of pipe breccias, S-N and SW-NE direction (Figure 3.1). These breccia complexes are up to several tens of meters in size, sometimes containing unalbitised fragments of psammite of about 0.1-1 m in size (Figure 3.3). The HA occurs predominantly along the hinge line of antiforms (Figure 3.1).

The medium intensity albitisation unit (MA) is characterised by grey and light brown colours of the affected lithologies and contains a group of breccia pipes striking in N-S (0-10°) direction, containing lenses of unalbitised metasediments of centimeter to meter scale. It should be noted that zones of intense albitisation can be found within zones of medium intensity albitisation although these were too small to mark in the scale map. These frequently occur in some small antiformal folds or small structures e.g. breccias, foliated structures and groups of faults. Figure 3.7 shows complete albitisation in MA with lines of crosscutting layers, foliated structure and antiformal folds.

The low intensity albitisation (LA) unit contains grey to dark grey coloured-rocks, with interlayered unalbitised metapelites including psammopelites and psammites from 20 centimeter to 1 meter thick (locally up to 10 m). The LA occurs close to or within synformal sections and includes biotite and minor muscovite alteration (Figure 3.4).

Based on composition and genesis, four specific lithologies within the three units outlined above were independently mapped.

Albitisation Map of Migmatite Creek, Weekeroo Inliers, Curnamona Province (6933 - III - N, Outalpa South)

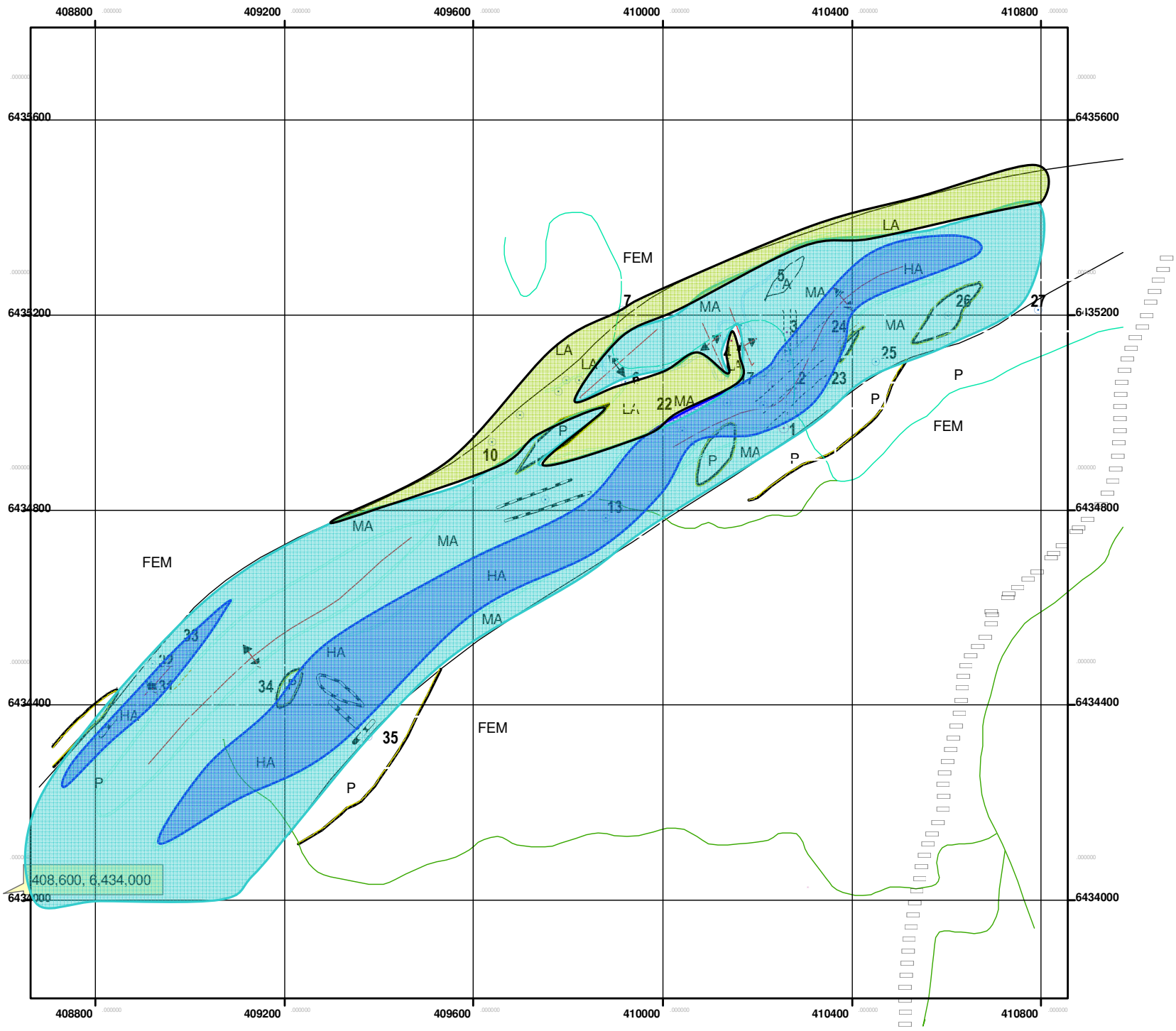

The Geocentric Datum of Australia (GDA94)

Cheng Lin Y. The University of Adelaide. June 2007.

REFERENCE

FEM Composite Gneiss+ Pegmatite Unit, Pelite - Psammopelite- rich Gneiss, four types of Pegmatite, and also albitisation and breccias inside in the south creek.

LA Low intensity albitisation zone, contains 50 to 100 % of Psammite, Psammopelite and Pelite.

MA Medium intensity albitisation zone, 45% to 65% albite. Contains north - south breccias and 20-30% of original Psammite, Psammopelite and pelite.

HA High intensity albitisation zone, 65% -100% albite. Contains 0 - 20% of MA and LA. Common network of breccias in both directions, N -S and 60+/- 10 degrees (Northeastern).

P Pegmatite units, four types of Pegmatite are distinguished. the white and brown, fine-medium-grains of Plagioclases +K-feldspar +quartz + muscovite +/- Biotite (2*5 mm) and the coarse - grains of them (5*30 mm).

A Small Amphibolite unit, foliated and relict igneous textures, contains muscovite and biotite (1*4mm).

Quartz veins, contain the big black tourmaline crystal (1*5 cm).

Geological boundary

Albitisation zone boundaries

Pegmatite boundary

Breccias and brecciated veins/pipes.

Folds and fold axies

4 Location of samples in point

Location of photos and boundaries

Rivers

Country road

Figure 3.1 Albitisation Map in Migmatite Creek, Weekeroo Inliers, Curnamona.

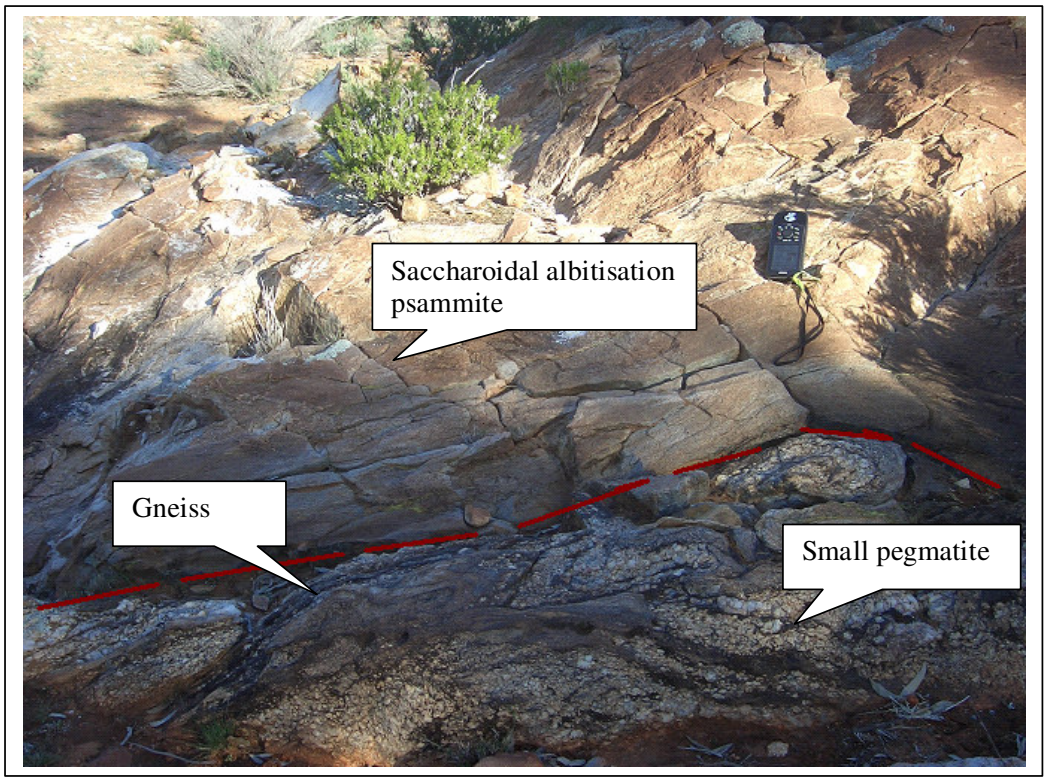

Figure3.2 The red line shows the boundary between FEM and the Plf.

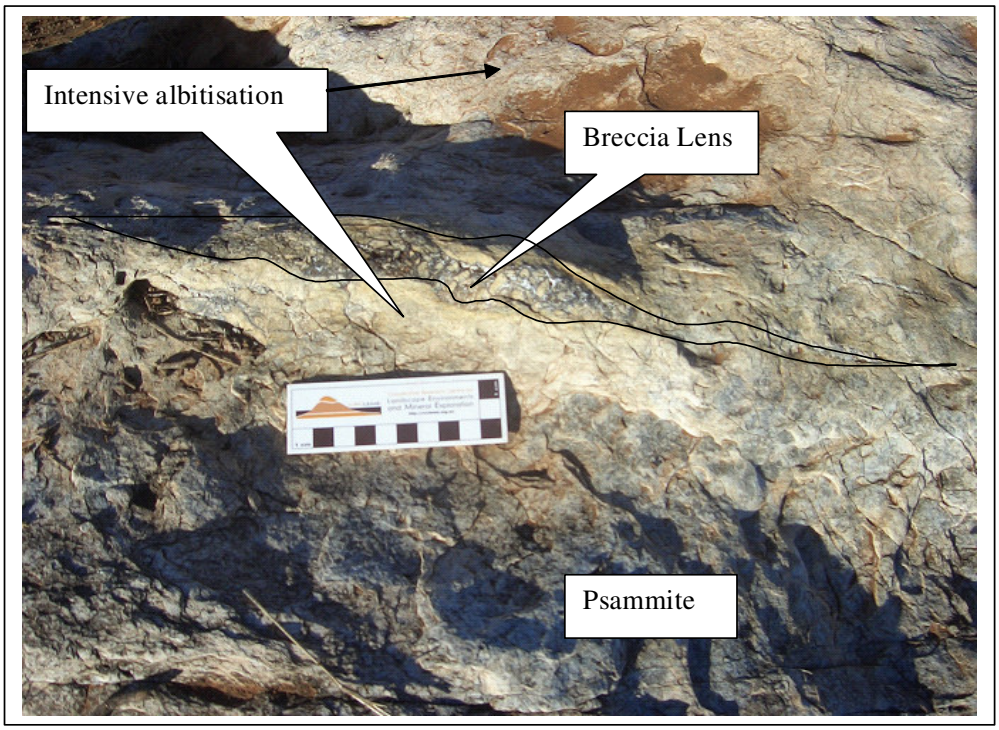

Figure 3.3 The breccia lens contains clasts of albitised rock and quartz and has mafic matrix support (point 17 of intensive albitised zone).

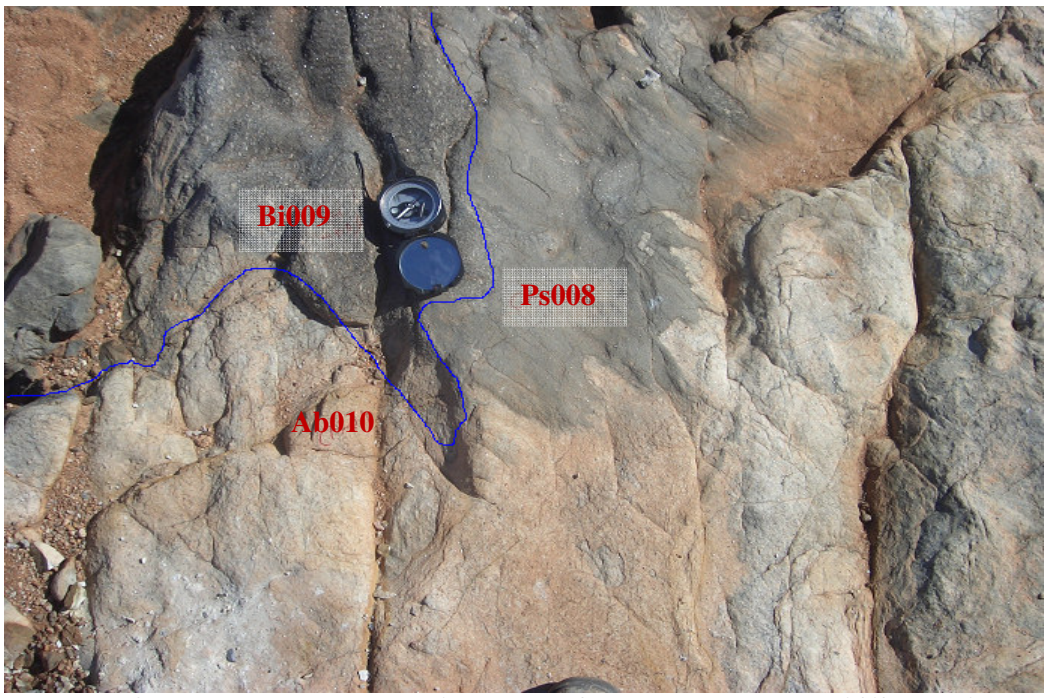

Figure 3.4 Showing variable intensity of albitisation (bottom part, sample Ab010); the left top part shows pronounced biotite alteration (sample Bi009) and the mid-top part is the original psammopelite / the least altered rock (Ps008) in sample point 4.

3.1.2 Distribution of the Lithological units

Metasediments comprise about 60%-70% of the area. Of these, psammite, psammopelite and pelite occur at about 70%, 20% and 10%, respectively. Metasediments include interlayered psammite and psammopelite; the apparent thickness of the metapelite unit is usually from 20 cm to 1 m and only exceptionally up to about 5 m so that three units could not be the distinguished at the used mapping scale. Furthermore, the three units change in mineral assemblages (quartz + feldspar + micas ± magnetite) with decreasing quartz content from the east to the west. Thus, psammite, psammopelite and pelite were not consistently differentiated in the mapping at the 1:10,000 scale.

Pegmatite, quartz veins and amphibolites, comprise about 30%-40% of the area. These units were marked using GPS data on the albitisation map. Breccias were partly marked on the map for the interpretation of albitisation.

Two boundaries between the units 'Plf' and the Migmatite 'FEM' were outlined in the map. The sampling and mapping emphasized on the variable intensities of albitisation. The map was built on scale of 1:10,000, using the ArcGIS program and produced on the Geocentric Datum of Australia (GDA 94).

3.1.3 Albitisation gradients in Pegmatites, Amphibolites and Quartz veins

Albitised pegmatite, amphibolite and quartz veins could be clearly identified in the field. Generally, albitisation of these lithologies resulted in white and light grey colours in contrast to the pink, brown and dark grey colours of the original rock. These are accompanied by albitisation of the surrounding metasediments at similar intensity.

Most of albitised pegmatite, amphibolite and quartz veins were less clear and had to be observed very carefully. There are more and larger pegmatites in the upper parts of the Plf than in the lower parts in the Migmatite Creek area. Two white types of pegmatite were albitised and two types of pink pegmatite could be the albitised or less albitised precursor (Figure 3.5). Albitised metasediments surround the pegmatites with gradual changes rather than sharp boundaries in colours, textures and mineral composition. Important was that albitised and unalbitised pegmatites could be distinguished based on their colour and mineral content (albite).

Amphibolite occurs within the MA unit and is surrounded by albitised metapelites. The foliated texture could be seen clearly in the amphibolite. The amphibolite also contains albitised zones along the foliated structures from mm to cm scales. Amphibolite has a layered or lens shaped appearance and may be described as the conformably intruded igneous body within metasediments parallel to the bedding at both the top and the bottom of it. Amphibolites are layered with distinct foliation and are also partly altered. The outcrop of amphibolite strikes in a direction of 70° (northeastern) with a width of 2 to 3m. The medium-grained, dark brown amphibolite is moderately but variably albitised intensity controlled by foliated structure or texture and porosity. Albitised amphibolite surrounds the less albitised centre at outcrop scale but the 0.2-0.5 cm visible albitised zones could be seen in spaceman in the centre (sample Am011).

Quartz veins occur in the vicinity of large pegmatites as well as albitic breccia bodies. They are suggested to represent the final stage of alteration as the result of Si saturation. Large quartz veins frequently occur in the upper parts of the sequence with big tourmaline crystals (up to 1×2×10 cm^3). Small quartz veins occur within the pegmatite bodies but do not cut into the albitised rock. The smaller quartz veins also occur within breccias (Figure 3.6).

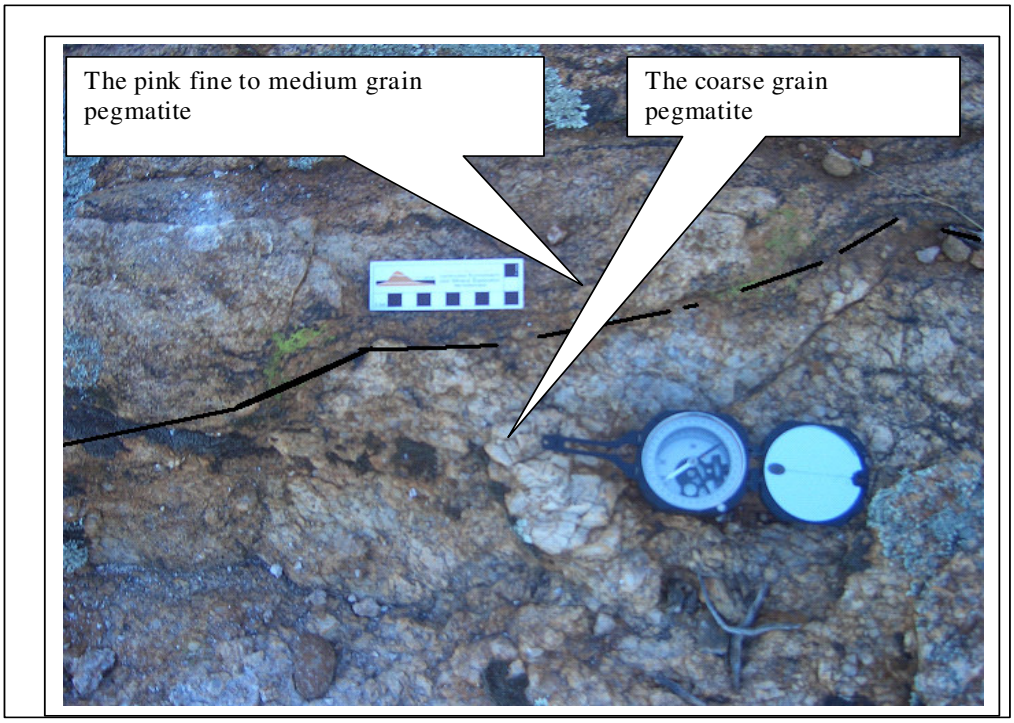

Figure 3.5 Two pink types of pegmatite: fine to medium grained (3-5mm) – and coarse grained (1-2cm), containing quartz, plagioclase (albite), K-feldspar and dark minerals (graphite) in point 26 with samples PB034 (albitisation) and PS035.

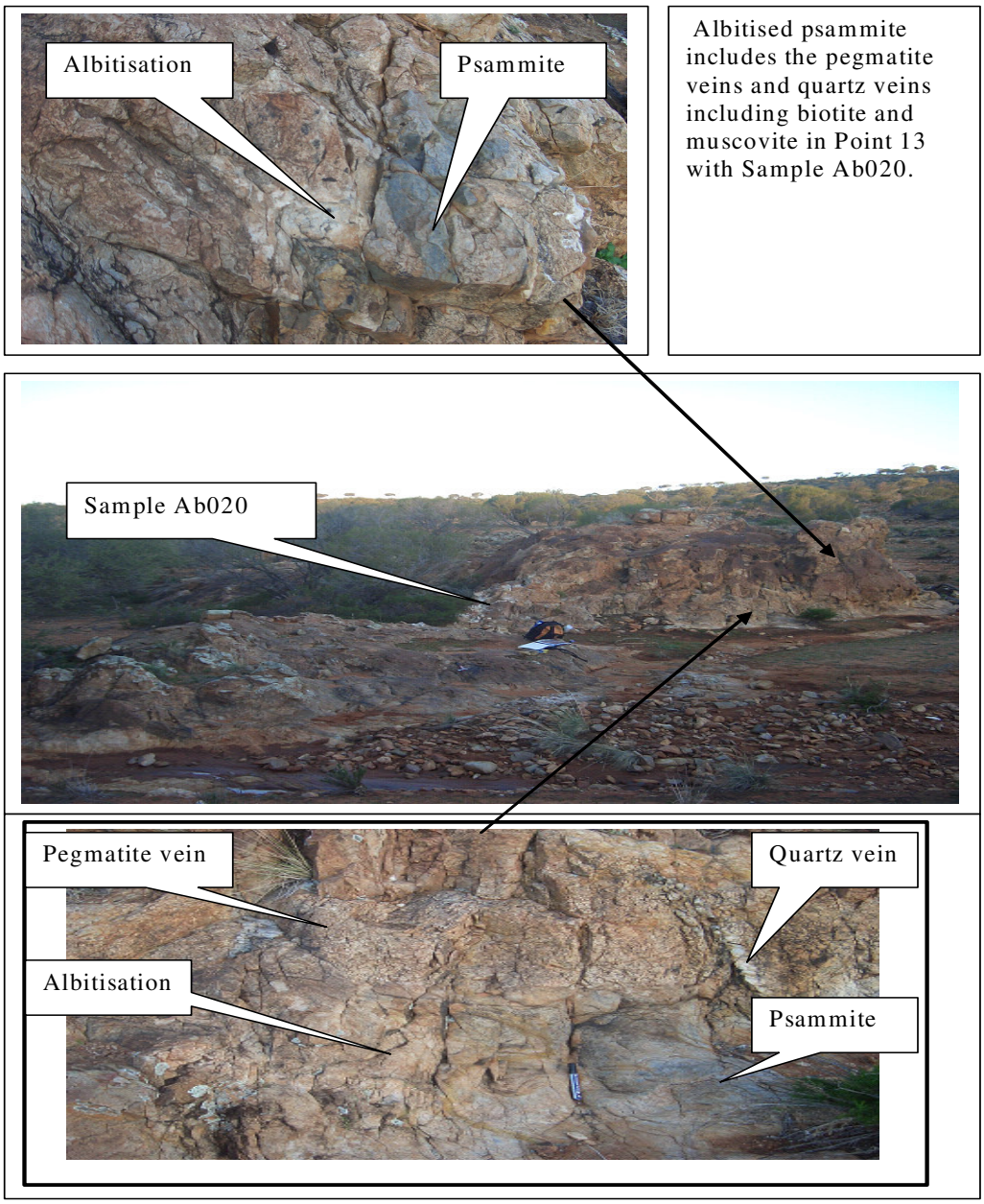

Figure 3.6 The large breccia body within a zone of intense albitisation, west of centre of mapping area. The central breccia body is surrounded by a network of smaller breccia pipes. Outcrop is in point 13 on Figure 3.1, sample Ab020.

3.2 Types of Breccias

Breccia occurrences broadly conform along strike of the main antiformal fold axial direction (45-65 degree, northeast direction, OD_3) and probably OD_2 linking to N-S (0-10 degree) direction (chapter 1.5.2). The breccias occur either within metasediment layers as small lens of 1.5 cm width and 10 cm length or as large breccia bodies of several meters width and more than 100 m length (Figures 3.3 and 3.6). Individual breccia bodies gradually increase in abundance from the east via the centre to the west.

The predominant type of occurrence of breccia in the area is as pipes and as networks. Breccia pipes are matrix supported in the centre and clast supported towards the margins containing rounded, sub-rounded or irregularly shaped clasts. Network type breccias contain a combination of the different breccias cutting the host lithologies at random angles. They are mostly matrix supported and all clasts are albitised.

The matrix supported cores of breccia bodies are about 10 to 20 m wide and 30-100 m long in the eastern section (Figure 3.6). The clasts consist of metasediments (psammite), pegmatite and quartz veins. The intensity of albitisation may decrease towards the centre of the breccias. The breccia body (Point 31 of the map) in the western section is also surrounded by breccia networks and matrix composition here is distinctly more mafic than that in east parts. Thus, the antiformal hinge zones comprise high intensity albitisation zones and contain several individual breccia bodies, possibly connected by a network of incipient brecciation/fracturing of the country rock.

3.3 Biotite Alteration and Silicification Alteration

Three types of alterations are distinguished in the area: i) albitisation, ii) biotite alteration and iii) silicification and quartz alteration. Biotite alteration occurs within metasediments apparently postdating albitisation (Figures 3.4 and 3.7). The biotite alteration occurs preferentially in the thinly layered albitised metapelites without associated breccias and unrelated to cleavages and faults. Biotite alteration is commonly associated with the intensive albitisation stage. Minor biotite alteration also affects the pegmatites and psammites (Figure 3.8) and could be seen to form small biotite-rich veinlets of 2-5 cm width.

Silicification and quartz alteration postdates both albitisation and biotite alteration in the form of small quartz veins/lenses along the boundaries between albitisation/biotite alteration and the metasediments/pegmatite (Figure 3.8). The light pink oil-lustre quartz veins are different from the early pure white quartz veins related to migmatization. The early quartz veins commonly contain large, black tourmaline crystals up to 10 cm length. Quartz veins or pegmatite derived from the migmatization are not visibly affected by biotite alteration.

Figure 3.7 Showing variable intensities of albitisation cross cutting OD3 deformation. The bottom part is albitised (MAb015) and the mid part is strongly albitised (HAb014). The top part is the biotite alteration (Bi013) and the boundary is along the fold axis.

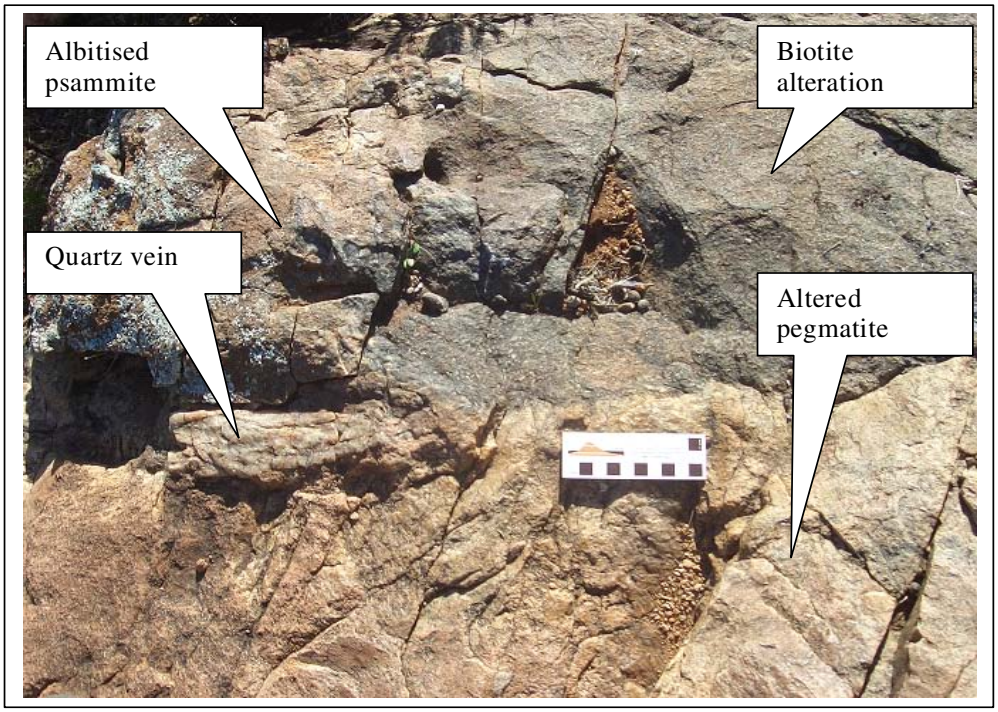

Figure 3.8 Showing boundaries, of biotite alteration/altered pegmatite, albitisation / biotite alteration and albitisation / altered pegmatite, associated with an OD3 fold axis. The small quartz vein cuts the boundary of albitisation/altered pegmatite in the intersection of the three alterations in location 24, samples Op031, Bp032 and BB033.

3.4 Analytical Results

3.4.1 Petrography

The Petrography was studied in field and with hand lens. The margins between unaltered and altered rock were clearly seen; and also the psammite, pelites, pegmatite, amphibolite, breccias and quartz veins were visibly identified. Albitisation and biotite alteration could be identified by studying the minerals albite and biotite in visible and under hand lens. The represent samples were taken from the margins of albitisation and biotite alteration, and the individual rock units. Based on lots of field description and specimen, the further lab micrographic sample pairs were prepared to study.

An initial set of 10 samples was taken to represent the 7 distinguishable rock types: pegmatite (MP001), breccias (B002, PB005), metasediments (L003, Uap007 and Ps008), high intensity albitisation (Ab004), medium intensity albitisation (Ab006), low intensity albitisation (Ab010) and biotite alteration (Bi009) in the Migmatite Creek area. Thirteen polished thin sections were made by Pontifex Petrographic Services and studied using a transmitted and reflected light petrographic microscope.

A second set of 13 samples was taken to represent the four levels of albitisation as well as biotite alteration, including HA (Ab004), MA (Mb006) and unalbitised psammite (Uap007). Low intensity albitisation is represented by a sample of albitised psammite (Ab010) sampled close to biotite alteration (Bi009) and the original psammite (Ps008). The second group of samples was taken to represent the albitised amphibolite (AbA012) and the unaltered amphibolite at the centre of the outcrop (Am011). A third group of samples represents biotite alteration (Bp032) and unaltered pegmatite (Op031). An additional fourth group of samples was to represent the various degrees of albitisation (MAb014, HAb015 and Ab021).

3.4.1.1 Lithologies

Metapsammite is the predominant lithological unit and comprises more than 70% rocks at the Migmatite Creek section that was studied. The mineralogical composition of the metapsammite comprises 30-60% quartz and 20-50% albite (plagioclase), 10-40% biotite (5-10% muscovite) (Figure 3.9), minor magnetite 0.5-3% is present in most samples. Accessory minerals are 1-5% garnet, amphibole, chlorite, pyrite, ilmenite and black rutile (Figures 3.10 and 3.11). Muscovite is an accessory in most lithologies but it is a major mineral in pegmatites. The grain size ranges from 0.2-0.6 mm and 0.025 to 5 mm for magnetite. The mineralogical compositions are consistent with whole rock data (Samples L003, Uap 007 and Ps008). Psammopelites and pelites were not sampled due to three reasons. Firstly, they were normally altered (albitisation and biotite alteration) without the appropriate primary unaltered pelites and psammopelites. Secondly, the outcrops of pelites and psammopelites were covered by regolith or soil because psammopelites and pelites were much stronger weathered than psammite. The weathered pelites and psammopelites were observed as the their relict fragments within soil with light yellow green colour, interlayered thin layers (2 mm to 2 cm thick within metapelites, 1 to 5 cm for psammopelites).

The high intensity albitisation zones (HA) consist of the predominantly albitised metasediments, breccias, networks of breccia pipes and pegmatite-quartz veins. In outcrop, the high albitisation units are a very clearly white, as distinctive from the light brown Medium Albitisation units. By using the stereo-microscope and petrographic microscope, the sample Ab004 of intensively albitised psammite comprises 70-80%

albite of 0.1-0.4 mm, 20-30% quartz, 5-10% biotite. 1-5% quartz occurs within the sugary albite as very fine grains. Accessory minerals are reddish brown rutile (TiO_2) 0.05-0.3mm, garnet 0.1mm, ilmenite ($FeTiO_3$) and black anatase (TiO_2) (Figure3.13). The accessory minerals and biotite are distributed along the crosscutting cleavage or microstructures.

The mineralogical compositions were 85-95% albite + 5-10% accessory minerals, quartz + micas + titanite/apatite in very intensively albitised psammopelite (sample MAb014).

The petrography of medium intensity albitisation zones (MA) consists mainly of the albitised metasediments, breccias, breccia pipes and amphibolites. In outcrop, the light brown MA units contain some lenses/layers of remnant psammite. In hand specimen, the albitised psammite is slightly reddish suggesting the presence of Fe^{3+}. Microscopically, in the sample Mb006, the medium albitised psammite comprises 60-70% albite, 10-30% quartz, 5-20% biotite (0.12-0.25mm) and 1-3% accessory minerals, ilmenite ($FeTiO_3$) and magnetite (0.03-0.07mm) (Figure 3.15). Magnetite is surrounded by biotite grown along the borders of minerals. The mineral assemblage is consistent with chemical compositions of sample Mb006 in medium intensity albitisation psammite.

The petrography of low intensity albitisation zones (LA) consists of the predominantly mildly albitised metasediments, biotite alteration of metasediments (pelites), and the metasediments. Low intensity albitisation zones are mostly mixed-units present along synformal hinges. In the field, the light grey LA units contain remnants of layer-scale psammite and biotite alteration. In hand specimen, the fine-grained, light grey, albitised psammite could also be observed to contain compact textures and parallel-layer linear textures defined by minerals. Microscopically, the sample Ab010 of albitised psammite comprises 50-60% albite, 20-30% fine-grain quartz, 10-30% micas (biotite) and 1-3% accessory minerals, magnetite, hematite and green malachite (Figure 3.16). Fine-grain quartz is distributed within the albite and biotite. Hematite is present in the centre of magnetite grains which are surrounded by primary biotite along the grain boundaries. The mineral assemblage was consistent with chemical compositions in sample Ab010 in albitised psammite.

Pegmatite is a complicated characteristic lithological unit in the mapping areas present predominantly in the upper part of Plf close to the FEM. It comprises 15-20% of outcrop in the area and its abundance decreases toward the lower part. It is presented in different sizes in different parts of the area. At least four types of pegmatite can be distinguished: i) coarse grained, white or light grey pegmatites, ii) fine–grained, grey to white pegmatites, iii) coarse grained, pink to light brown pegmatites, and iv) fine–grained, pink to light brown pegmatites (Figures 3.5 and 3.8). Pegmatite bodies are commonly variable in the range of 1–20 m width but small crosscutting pegmatite veins were seen in a specimen. Type i) is the dominant pegmatite within the mapping area. The mineralogical compositions consist of 10-30% quartz, 25% plagioclase (albite), 10-20% K-feldspar (up to 70% feldspars), 10-15% biotite, 30% muscovite and tourmaline. The mineral grain size was in the range of 0.5-1cm and quartz is of quite small grain size. Graphite could be found in pegmatites. Additional/accessory minerals are magnetite, apatite and possibly barite. Type iii) and iv) may be influenced by the Fe^{3+} ions-rich. Type iii) has been albitised against iv) (Figure 3.5)

The marginal albitisation zone of the amphibolite includes remnants of unaltered amphibolites (sample AbA012). The mineralogical composition of amphibolite comprises the 30-40% anthophyllite, 5-10% hornblende, 10-40% magnetite, 15%-20% albite, 20% plagioclase, 10-20% biotite/muscovite and 1-30% quartz (Figure 3.13). The

grain size of minerals is in the range of 1-4 mm except quartz (down to 0.04 mm) and magnetite (up to 7 mm). Fine crystals of Al-Anthophyllite (Ferri-Gedrite) are present within cavities of magnetite or the borders (Figure 3.13). Micro-albitisation zones are clearly present in the centre of amphibolite (Am011) and they are more than the margins of albitised amphibolite (AbA012) unexpectedly.

Biotite alteration of metasediments (Bi009) has a mineralogical composition of >50% micas (30-40% biotite + 10-20% muscovite), 20-30% albite, 5-25% quartz with minor minerals, 5-10% magnetite, 1-5% garnet (0.1mm) within biotite, and accessory fine rutile 0.5% (yellow pink).

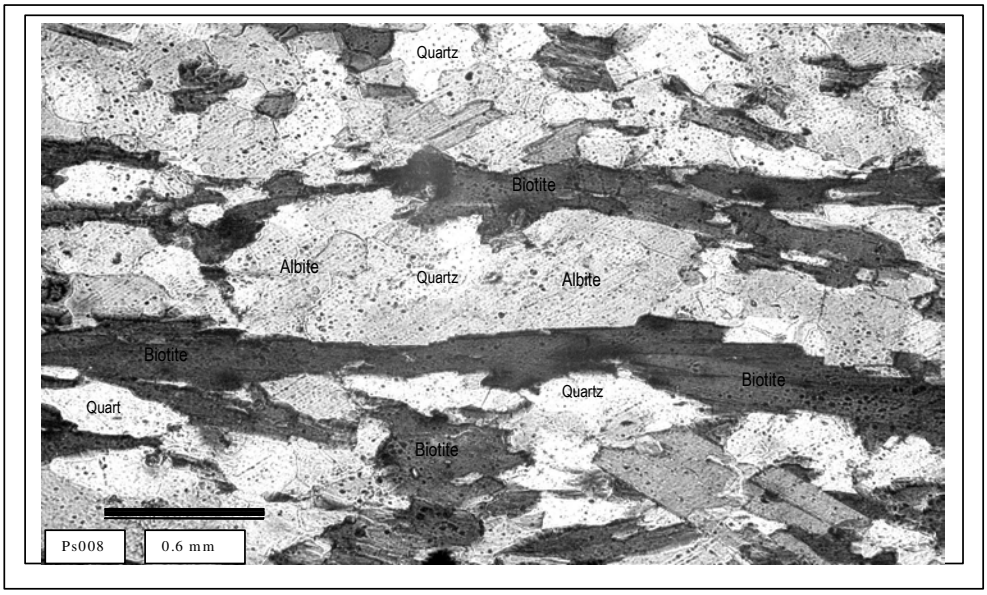

Figure 3.9 Unaltered psammite has quartz + albite + biotite ± magnetite assemblage (sample Ps008).

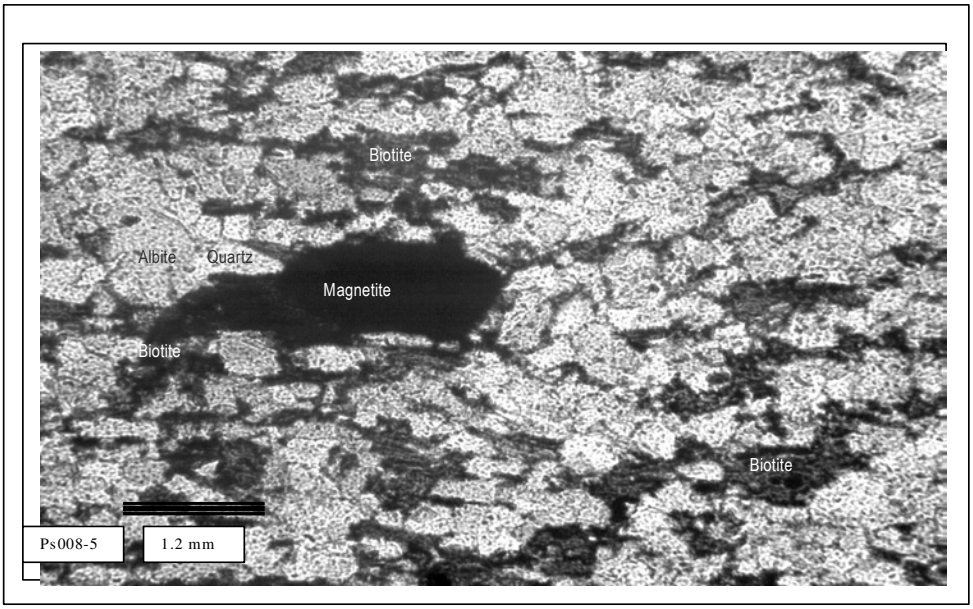

Figure 3.10 Unaltered psammite has quartz + albite + biotite + magnetite (sample Ps008).

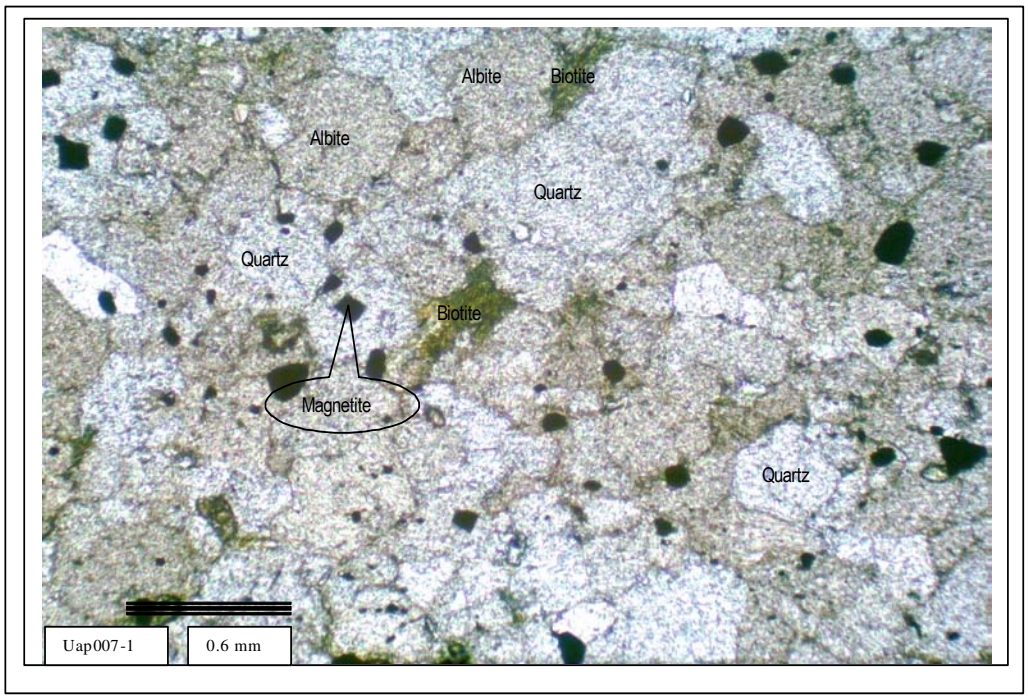

Figure 3.11 The least altered/unaltered psammite has quartz + albite + biotite + accessory assemblage magnetite (sample Uap007).

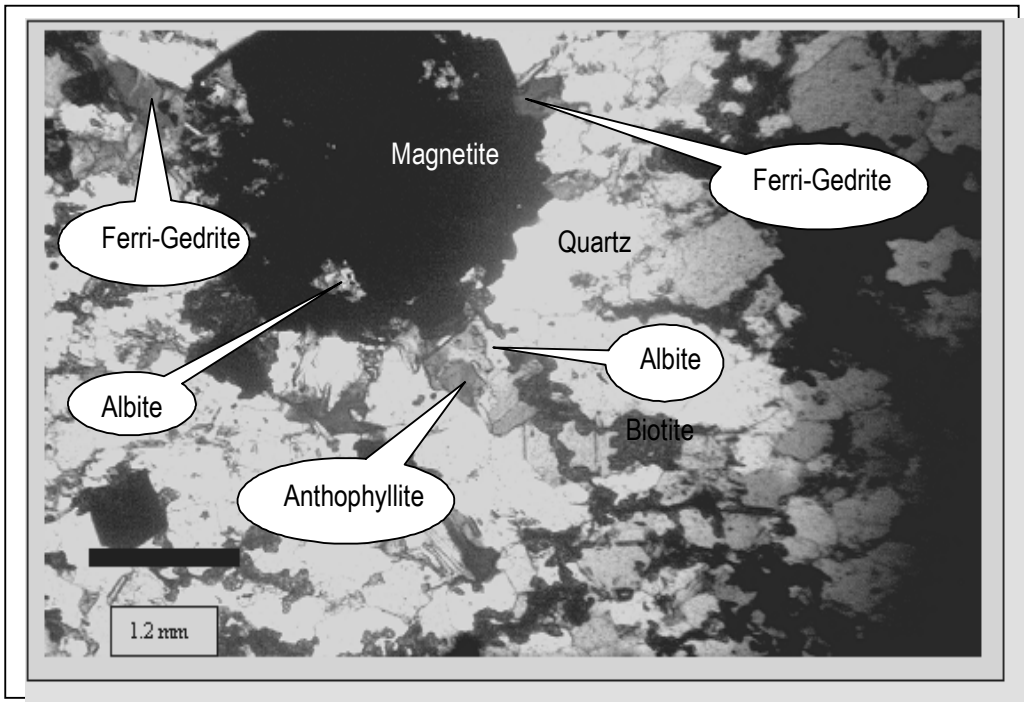

Figure 3.12 The albitised amphibolite has magnetite + anthophyllite (ferri-gedrite) + micas + quartz (sample AbA012).

3.4.1.2 Mineral phases/generations

The entire original mineral assemblage is replaced by albite during high and medium intensity albitisation (Figures 3.13 to 3.16). The new secondary mineral assemblage was then established as albite + quartz ± accessory minerals (micas ± magnetite ± titanite ± apatite). Albite is usually of large grain size (0.6-1.2 mm) while quartz, magnetite and accessory minerals are of small grain size (0.1-0.3 mm). Quartz and biotite are extremely decreased in secondary mineral assemblages. Figure 3.15 shows that the secondary mineral phase is very close the equilibrium but the shade shapes of biotite were clearly observed as the possibly remained phase.

Micas are present in most lithologies. Biotite is most common in metasediments, pegmatites and amphibolites and is the predominant mineral in biotite alteration units. Biotite is present at three generations of different genetic origin. For convenient reason, the first generation of biotite was derived from the metamorphism, migmatization and igneous processes. The second generation of biotite was derived from the hydrothermal event (OD_3) during or just after the albitisation processes. The third generation was from high intensity biotite alteration.

The timing of biotite was identified from field and micro observation. The first generation linked to low or at least albitisation or without. The second generation formed at the same processes with albitisation as co-existing in the MA. The third generation close to the HA or cut the albitisation units.

The first generation of biotite could be seen as pseudomorphs or relict parts in albitised rock. Biotite is predominantly euhedral to subhedral in sizes of crystals of 0.2–1 mm in metasediments (samples Ps008, Uap 007), amphibolite (Am011) and pegmatite (Op031) (Figures 3.9 to 3.11). The mineralogical compositions are variable in the range of about 10-45% micas (biotite + muscovite) in these rocks. Increases of muscovite are observed in the pegmatites and the amphibolites in both, the content and the size of individual mineral grains.

The second generation of biotite is predominant anhedral in albitised metasediments (samples Ab004, Mb006 and Ab010) and the albitised amphibolite (AbA 012) (Figures 3.13 to 3.16). The second generation of biotite has variable sizes of 0.05-0.2 mm. This may mean that both the replacement reactions and the re-forming biotite are possible. Multiple chemical equilibria are albite + quartz ± biotite in fluid/rock reactions. The major mineral assemblages are changed form quartz – biotite - albite to albite – quartz. Albite replaced most of biotite as well as remaining accessory minerals (Figure 3.12 to 3.16). The secondary mineral phases are the new mineral assemblages although relict minerals remain of some primary mineral phases due to incomplete chemical equilibrium/reaction.

The third generation of biotite is present in biotite alteration of both psammite (sample Bi009) and psammopelite (Bi013). Biotite alteration of metasediments (Bi009 and Bi013) consists of 50-70% biotite or more. They are present as anhedral crystals with sizes of 0.5-5 mm and accessory subhedral aggregates. The sizes of biotite are consistent at about 1 mm diameter in the altered pelites and psammopelite (metasediments).

The distribution of magnetite is dependent on the types of lithologies. Magnetite is a common minor mineral in all lithologies and a major mineral in the amphibolite. The amphibolite has the highest content of magnetite at about 10–30% in the size range of 0.04 to 5 mm (Figure 3.12). Psammite contains fine to medium grained, brown magnetite in the range of 1-5%. The pegmatites have the least magnetite (<1%) at the smallest grain size. In thin section magnetite occurs as irregularly shapes and in linear

arrays along foliation. The opaque minerals were studied in both, stereo-microscope and polarized microscope. Magnetite in linear distribution was clearly identified in hand specimens and thin sections with euhedral crystal shapes in amphibolite. Individual crystallites of magnetite are partly replaced by albite and micas (Figure 3.12).

In metasediments, the size of magnetite grains is normally between 0.5 and 2 mm diameter (samples Uap007, Ps008 and L003) (Figures 3.9 and 3.11). Magnetite occurs in the light grey low albitisation rock as single mineral grains of small sizes (0.04–0.5 mm) and also in fine linear microstructures. In medium intensity albitisation rock, the range of sizes of magnetite increases to 0.04–1 mm with increasing porosity but the total content of magnetite is less than that in low intensity albitisation rocks. In high intensity albitisation rocks, the fractured microstructures strongly increase with the size of individual magnetite grains but overall magnetite content decreases.

The primary and secondary mineral phases were very complicated in the centre of amphibolite and the edge of albitised amphibolite. In general, the sizes of magnetite are in a narrow range of 0.2-2 mm in Am011, and in AbA012 the distribution are bimodal, 0.05-0.2 mm and 3 mm-1 cm. The coarse grains (1 cm) of magnetite align in foliated direction or linear microstructures as strings of beads in amphibolite. Numerous holes within large magnetite grains (1 cm) are filled by other minerals. These magnetite grains have the irregular grain boundaries fractured or replaced by other minerals grains. Newly formed magnetite is of distinctly smaller grain size to 0.01 mm, euhedral crystal shape, and of irregular distribution or occurs as inclusions in other minerals. Dissolution partly occurred in the centres or along the grain boundaries of magnetite during albitisation (Figure 3.12).

Quartz is present in all lithologies. In the metasediments, coarse or fine-grained quartz is observed in both, hand specimen and outcrops. The coarse-grained saccharoidal quartz occurs in albitised psammites at the top part of Plf contacting to the bottom of FEM. Coarse-grained, white quartz veins occur in pegmatite bodies, breccias and along rock boundaries. These quartz veins likely formed during the final stage of albitisation and biotite alteration.

Accessory minerals are garnet, tourmaline, graphite, ilmenite, rutile, hematite, pyrite, barite, zircon, titanite, apatite and possible fluorite. The primary accessory minerals, for example garnet, chlorite, pyrite, ilmenite and black rutile almost completely disappeared during albitisation, except in Al-Anthophyllite (ferri-gedrite). Tourmaline, graphite and hematite were clearly observed in the outcrops and hand specimens. Disseminated hematite (or oxidised Fe ion) or magnetite occurs in the MA zones in metasediments and resulted in the red colour in the whole MA. Disseminated hematite is also common in the large breccia bodies. Garnet, ilmenite, rutile, pyrite, zircon were identified microscopically. Euhedral garnet crystals of 0.1 mm diameter are present within the large euhedral biotite crystals in sample Bi009. Small zircon crystals were observed in sample Bi009 and PB005 using the Stereo-Microscope. Euhedral crystals of ilmenite and black rutile were determined in range of 0.05-0.1 mm size in sample Ab010. Crystals of 0.05 mm grossular $Ca_3Al_2(SiO_4)_3$ were found in the MA unit (Ab006). Pyrite was only determined in one psammopelite sample (Uap007).

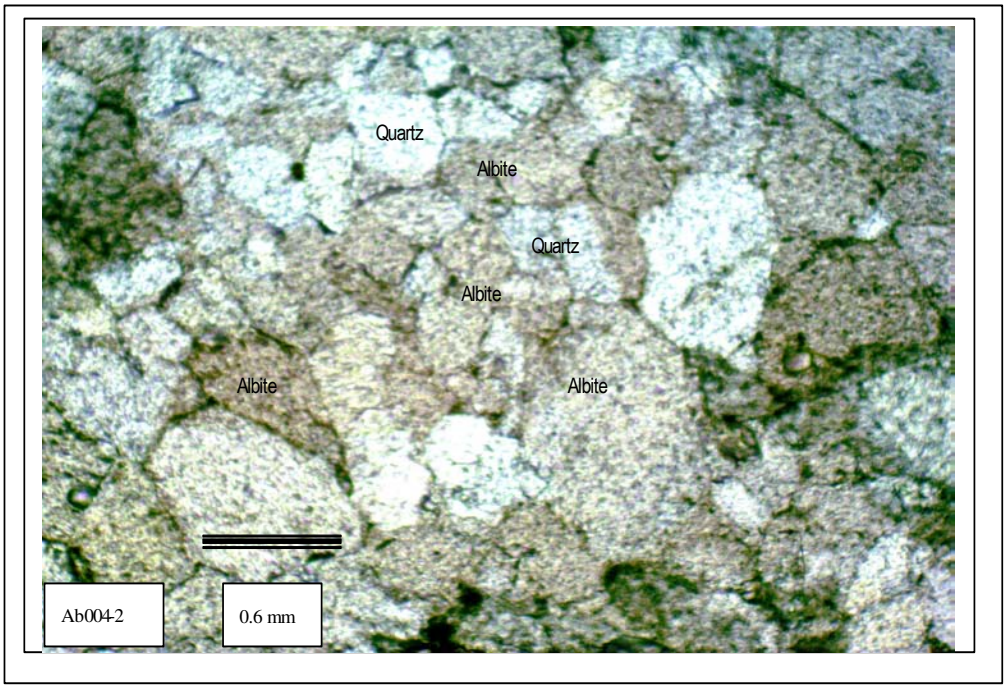

Figure 3.13 Albite + quartz + biotite in intensely albitised psammite (Ab004).

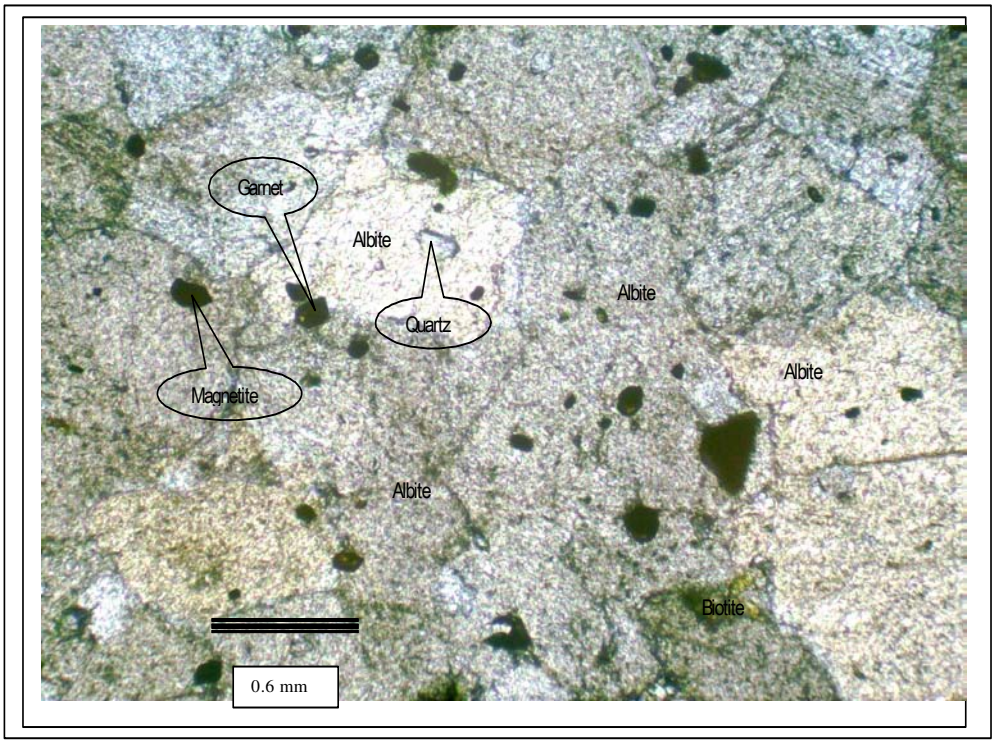

Figure 3.14 85-95% albite + quartz + micas + titanite/apatite in very intensely albitised psammopelite (sample MAb014).

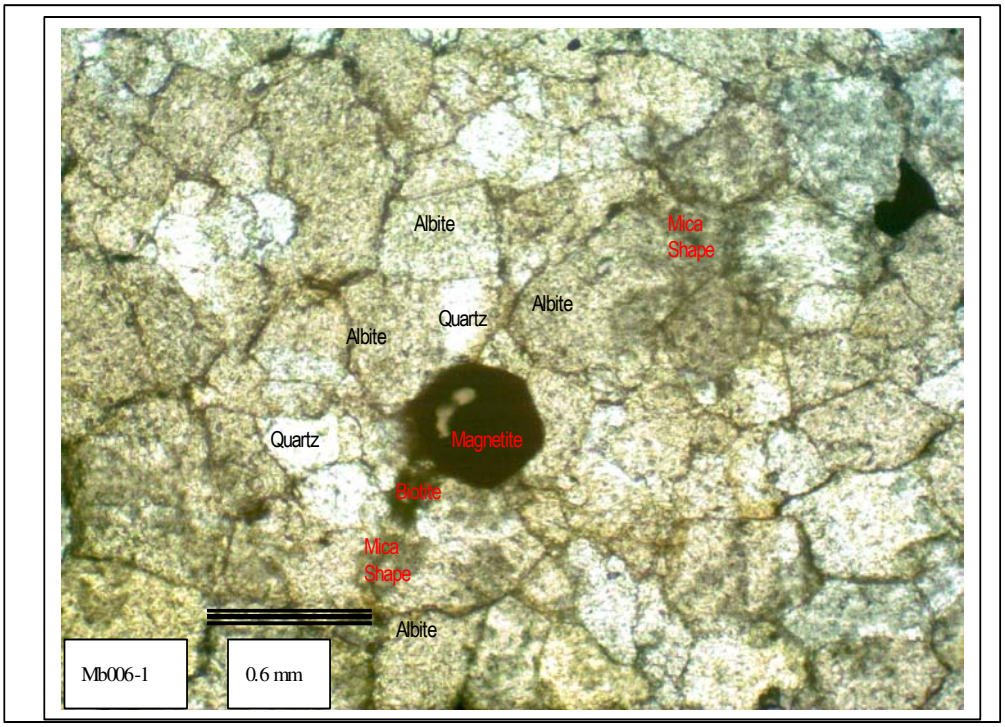

Figure 3.15 Albite + biotite + quartz + magnetite in medium intensity-albitisation psammite (sample Mb006).

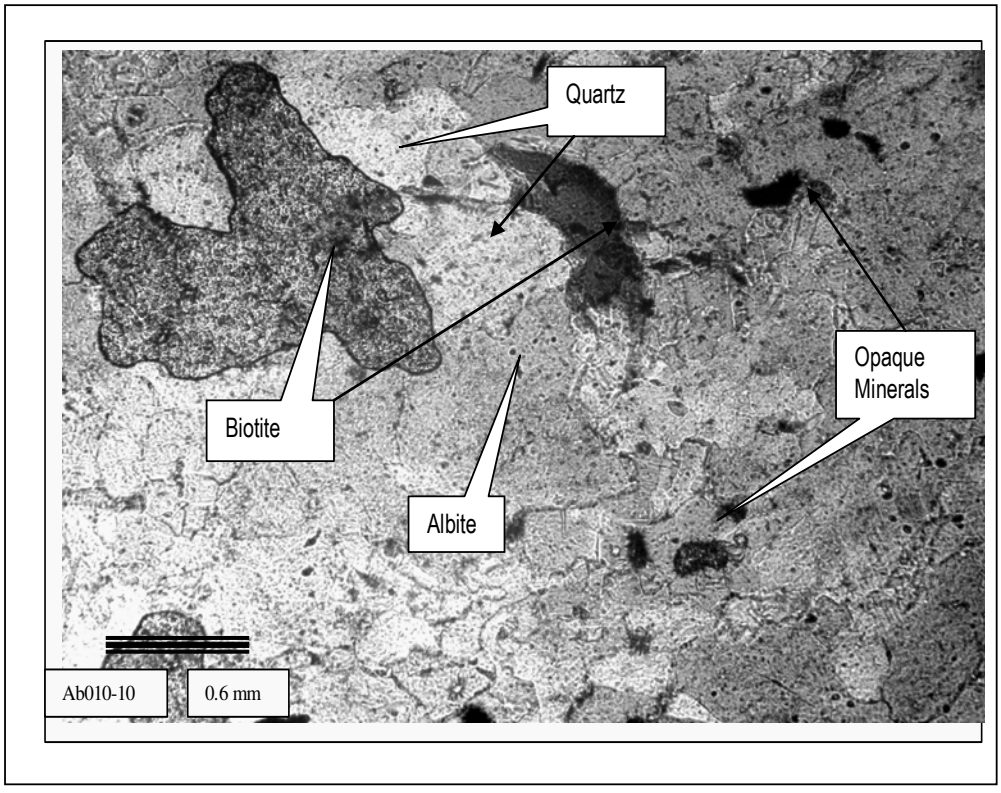

Figure 3.16 Albite + biotite + quartz + magnetite in low albitisation of psammite (sample Ab010).

3.5 Whole Rock Analysis

3.5.1 Whole Rock Compositions

Samples of all lithologies were analysed for their major, trace and REE compositions. Major elements as well as selected trace elements were determined using the Adelaide university XRF facility (see appendix B-1). Due to a breakdown of the XRF instrument further analyses were carried out through a commercial provider (AMDEL) using total digest ICP MS method (for details of the analytical procedures see appendix B-2).

A total of 41 samples were taken to represent the rock types present. For a first order distinction of different intensities of albitisation, the analytical results were plotted in ternary diagrams of Na_2O-K_2O-CaO. The ratios of CaO/(Na_2O+K_2O+CaO) are < 0.05 in pegmatites, breccias, metasediments and the variably altered rock samples (Figure 3.17). Three samples, one of each of amphibolite, the albitised metasediments and the biotite alteration of metasediments, were in the range of 0.05-0.11 of CaO/(Na_2O+K_2O+CaO) ratios. Thus, lack of CaO was clearly identified in all rock sequences in the mapping areas. In pegmatites (8 samples), the ratios of Na_2O/(Na_2O+K_2O+CaO) ranges from 0.32 to 0.73 and the ratios of K_2O/(Na_2O+K_2O+CaO) were little lower in the range of 0.21-0.63. This means that the Na_2O/K_2O ratios are commonly 0.5-3.5 in the pegmatites. In most cases the Na_2O/K_2O ratios are in the range of 2–60 in metasediments, amphibolite and albitised rock. However, low Na_2O/K_2O ratios of 2-3 were determined for biotite alteration of psammite or psammopelite.

The composition ranges of metasediments (psammite) are 3.5-5 wt% Na_2O, <2 wt% K_2O, 6.5-12 wt% Al_2O_3 and 0.5-3 wt% Fe_2O_3. The chemical composition of psammite (samples L003, Uap007 and Ps008) is rich SiO_2, low MnO and CaO (Table 4). The 76.78–86.45 wt% SiO_2 represents 10-30% quartz; anorthite was not identified, in agreement with only 0.01-0.03 wt% CaO in psammite. The 0.21-0.31wt% TiO_2 in psammite was consistent with the accessory ilmenite and rutile.

The chemical composition of sample Ab010 (LA) comprises Na_2O 6.37 wt% (57% albite), SiO_2 76.73 wt%, Al_2O_3 12.34 wt%, Na_2O 6.37 wt%, K_2O 0.50 wt%, and Fe_2O_3 0.44 wt%. It is characterised by low MnO, MgO, CaO and P_2O_5 (total <0.4%) and high Y concentration (188.3 ppm) (Table 4).

The composition of sample Mb006 (MA) has 7.71 wt% Na_2O (68.91% albite), 77.01 wt% SiO_2, 13.64 wt% Al_2O_3, 0.98 wt% Fe_2O_3. It is also characterised by poor MnO, MgO, CaO and K_2O (total <0.4%). It characterised by high concentration of Zr 405.4 ppm and low concentration of Ba 26 ppm (Table 4).

In MA, completely albitised psammopelite was found in samples MAb014 and HAb015 despite lack of unalbitised psammopelite in the outcrop (Figure 3.6). Its chemical composition comprises 10.1-10.3 wt% Na_2O (85-95% albite), 67.1-67.4 wt% SiO_2, 18.1-18.5 wt% Al_2O_3 and 0.86-2.94 wt% Fe_2O_3. It is characterised by low concentrations of Mn (<0.01 wt%), Ba (20-50 ppm) and U (0.44–0.53 ppm) (Table 4).

The chemical composition of sample Ab004 (HA) comprises 8.6 wt% Na_2O (76.86% albite), 74.99 wt% SiO_2, 15.14 wt% Al_2O_3. It is characterised by high concentration of Zr 405 ppm and low concentration of trace elements (Table 4).

The chemical composition of pegmatite (Mp001, Pm017, Op031 and Ps035) is SiO_2- rich (73.24–83.2 wt%) and low in MnO (0.01-0.02 wt%) and CaO (0.08-0.23 wt%) (Table 4), 1.77-4.73 wt% Na_2O and 1.52-5.85 wt% K_2O and is consistent with the observed quartz - albite – orthoclase – mica assemblage. The chemical compositions of

altered pegmatite (sample Bp032) consist of major elements: 80.48 wt% SiO_2, 9.65 wt% Al_2O_3, 3.89 wt% Na_2O, 0.30 wt% MgO, 1.16 wt% Fe_2O_3, 1.62 wt% K_2O, 0.07 wt% CaO, 0.15 wt% TiO_2, MnO 0.01 wt%, 0.04 wt% P_2O_5. The chemical compositions of sample Bp032 demonstrates that biotite alteration is at quite low level compared to intense Si-alteration, representing biotite and Si-Fe-Mg alteration.

The chemical composition of amphibolite is Fe_2O_3-rich (23.20 wt%) and poor in MnO – CaO (Table 4). MgO and Fe_2O_3 contents are related to the magnetite – Al-anthophyllite – albite - biotite assemblage. 0.34 wt% TiO_2 and 0.18 wt% P_2O_5 can be related to accessory titanite and fluorapatite. The total REE contents are respectively 160 ppm in sample Am 011 and 139.32 ppm in sample AbA012 (Table 5).

Chemically the breccias (samples, B002, PB005, BAB023, BB033 and PS040) are rich in SiO_2 and Na_2O but poor in CaO (Table 4). The compositions are consistent with mineral assemblages. 578.6 ppm Zr in sample PB005 is in agreement with the observation of zircon grains (see Chapter 3.5.1).

The chemical compositions of biotite alteration of metasediments (samples Bi009 and Bi013) comprises low SiO_2 concentrations (57.18–61.20 wt%) and high contents of Fe_2O_3 – MgO - TiO_2 (Table 4). This is in agreement with the observed mineralogical compositions of >50% micas (30-40% biotite + 10-20% muscovite), 20-30% albite, 5-25% quartz, minor minerals, 5-10% magnetite, 1-5% garnet (0.1mm) as well as accessary rutile (0.5%). The total REE contents are respectively, 186.51 ppm in the biotite alteration of psammopelite (Bi013) and 70.24 ppm in the biotite alteration of psammite (Bi009).

The concentrations of Fe_2O_3 are variable in the samples of albitised metapsammite Ab004 (Fe_2O_3 0.14 wt%), Mb006 (Fe_2O_3 0.98 wt%) and Ab010 (Fe_2O_3 0.44 wt%).

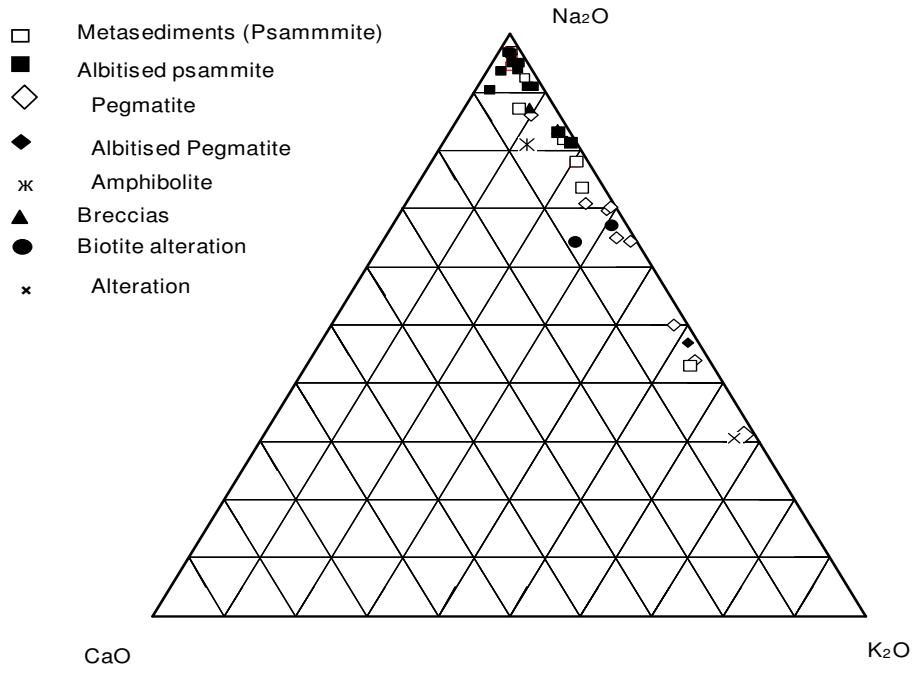

Figure 3.17 CaO-Na_2O-K_2O normative contents of all samples, see legend for rock types. The rock types are pegmatite, breccias, metasediments, amphibolite, albitisation, alteration and biotite alteration. The ternary plots show the Na_2O rich nature, the general lack of Ca in all rock types and low K content except pegmatite and biotite alteration from whole rock data of 41 samples.

Table 4 Whole rock data (XRF and ICPMS) represent the original and the altered rock types.

Rock type	Pegmatite	Breccia	Psammite	Albitised psammite	Albitised psammite	Albitised psammite	Albitised psammopelite	Biotite alteration metasediments	Amphibolite
Sample Name	MP001 Pm017 Op031 Ps035	B002 PB005 BAB023 BB033 PS040	L003 Uap007 Ps008	Ab004 (HA)	Mb006(MA)	Ab010(LA)	HAb014 Mab015	Bi009 Bi013	Am011 Aba012
Major elements (wt.% oxides)									
SiO2	73.24–83.2	74.7-84.46	76.78-86.45	74.99	77.01	76.73	67.1-67.4	57.18-61.20	62.4-63.1
Al2O3	8.72-15.04	7.44-13.4	6.64-11.48	15.14	13.64	12.34	18.1-18.5	14.99-17.51	7.41-7.67
Fe2O3T	0.16–3.55	0.32-3.07	0.55-2.72	0.14	0.98	0.44	0.86-2.94	4.53-8.39	22.3-22.9
MnO	0.01-0.02	0.01-0.03	0.01-0.03	0.01	0.01	0.01	<0.01	0.05-0.09	0.04-0.05
MgO	0.08-1.11	0.16-1.69	0.13-2.02	0.04	0.01	0.16	0.01	4.77-6.01	1.52-2.28
CaO	0.08-0.23	0.09-0.19	0.05-0.22	0.14	0.14	0.13	0.46–0.85	0.22-0.59	0.28-0.3
Na2O	1.77-4.73	3.13-5.99	3.70-4.83	8.60	7.71	6.37	10.1-10.3	4.47-6.75	2.6-3.16
K2O	1.52-5.85	0.20-1.57	0.07-1.55	0.14	0.12	0.50	0.23-0.26	1.87-3.12	0.45-0.67
TiO2	0-0.54	0.11-0.58	0.20-0.31	0.20	0.15	0.14	0.665–0.96	0.31-0.81	0.28-0.335
P2O5	0.1-0.19	0.02-0.16	0.02-0.07	0.01	0.01	0.02	0.15–0.55	0.02-0.34	0.16-0.19
SO3	0.01	0.00-0.01	0.01-0.02	0.00	0.01	0.01	-	0.01	-
LOI	0.11-0.53	0.16-1.39	0.13-0.43	0.08	0.13	0.35	0.41-0.47	0.65	0.63-0.64
Total	98.5-99.70	99.6-100.5	99.67-100.15	99.48	99.90	97.19	99.78-99.85	99.13	99.06-100.3
Trace elements (ppm)									
Sc	0.2-16	3.7-10.0	1.7-4.9	3.2	1.5	1.5	<5	11.5-14	<5
V	6-40	9-33	21-26	9	13	8	50-70	35-80	70
Cr	9-80	0-7	7-37	4	3	4	50	2-80	30-40
Co	69-100	36-86	32-52	23	26	45	27-32.5	20-315	21.5-52
Ni	<2-21	1-20	2-14	0	1	2	<2	36-62	5-6
Cu	2.5-8.5	3.5-50	-	-	-	-	2.5-6	3	2-7.5
Zn	1-34	7-54	1-19	1	0	0	<0.5	46-105	50-58
W	900-1050	490-550	-	-	-	-	310-360	240	220-500
Ga	11-20	19.6-28	9.3-17.7	23.1	26.9	18.1	21.5-24	29.5-39.9	14.5-16

Rock type	Pegmatite	Breccia	Psammite	Albitised psammite	Albitised psammite	Albitised psammite	Albitised psammopelite	Biotite alteration metasediments	Amphibolite
Rb	31.5-155	7.0-72	2.1-44.6	4.1	2.9	9.3	1.3–1.7	91.6-110	18.5-32.5
Sr	19-40.1	7.2-21.5	11.8-16.3	21.3	21.6	20.6	16–24	22.5-31.5	15-31.5
Y	7.4-19	32.5-363.9	31.1-129.4	75.7	115.3	188.3	1.65-4.4	10.5-110.0	7-8
Zr	4.5-390	270-578.6	201.7-371.0	405.0	405.4	329.4	230–310	190-621.5	90-120
Nb	1.8–16	2-162.6	7.4-67.8	67.3	97.0	66.8	7.5–10.5	6.5-83.2	<0.5
Ba	150-885	40-240	57-131	21	26	125	20-50	110-206	30-40
Th	2.0-26.5	33.5-47	8.3-34.9	42.7	48.5	33.8	7–9	23.5-47.6	9-10.5
U	0.5-21	3.6-87.9	1.6-11.8	3.4	7.4	3.3	0.44–0.53	3.6-12.0	2.9-4.2
Pb	13.7-16.5	3-7.5	3.2-5.2	4.3	4.6	3.9	2.5–3	3-5.8	2-6
La	0-30.5	1-72	20-87	0	3	0	2.5-3	3-40.5	31-36.5
Ce	5-70	16-170	58-201	4	17	7	4.5-6	17-84	62-74
Nd	0-28.5	10-80	33-105	3	16	3	3.1	6-34	25-28.5
REE									
Pr	0.1	1.45-19	10-43	0.3	L.N.R.	0.4	0.65-0.67	2.1	6.5-7.5
Nd	0.47	7-80	42-160	2	L.N.R.	2.2	3.1	10	25-28.5
Sm	0.17	3.8-19.5	11.5-28.5	1.55	L.N.R.	1.6	0.75-1.1	4.2	5.5
Eu	0.07	1-3.2	1.75-3.1	0.39	L.N.R.	0.35	0.2-1	0.84	0.8-0.83
Gd	0.15	6.5-18.5	11.5-17.5	2.3	L.N.R.	2.7	0.55-1.2	6	3.4-3.6
Tb	0.04	1.75-4	1.15-2.2	0.72	L.N.R.	0.77	0.09-1.2	1.45	0.44--0.48
Dy	0.21	11-24	4.5-11	4.3	L.N.R.	5	0.45-1.05	9	2-2.2
Ho	0.05	1.95-4.3	0.81-1.95	0.82	L.N.R.	1	0.08-0.18	1.7	0.31-0.33
Er	0.15	6-13.5	2.6-6	2.7	L.N.R.	3.6	0.25-0.6	6	0.9
Tm	<0.05	0.85-1.9	0.35-0.85	0.4	L.N.R.	0.5	<0.05-0.1	0.9	0.1
Yb	0.45	6-13.5	2.3-6	2.8	L.N.R.	3.7	0.35-0.75	7	0.75-0.8
Lu	0.03	0.83	0.33-0.88	0.39	L.N.R.	0.56	0.05-0.13	1.05	0.11-0.12

Note: Rare Earth Elements of 10 samples (Mp001-Ab010) were analysed by IC3R in Amdel Limited and the rest was analysed by XRF in the Mawson Laboratory. All element of 31samples (Am011-Ap042) was analysed by Amdel Limited.

3.5.2 Whole Rock REE Compositions

All samples were analysed for their REE contents by Amdel (see Chapter 2.3 for methods) but one powder sample (Mb006) was lost during delivery. REE values were normalised to ordinary chondrite (White 2006) using the GCDkit 2.2 program package. The total REE content is in the range of 6.89 ppm (pegmatite Mp001) to 618 ppm (psammite LCS029) (Table 5). The REE patterns have a negative Eu anomaly in all rock types with the exception of one sample (Mp001). In albitised psammite the negative Eu anomaly is accompanied by a positive Ce anomaly (Figures 3.18A). The light REE has the stronger depletion than the HREE has.

The total REE contents are respectively present in the range of 183.63–618 ppm with the average 367.92 ppm in 4 samples of the metasediments, and in the range of 15.54–247.07 ppm with the average 56.71 ppm in the albitised metasediments (La and Ce were analysed by XRF and Pr, Nd, Sm, Eu, Gd, Tb, Dy, Ho, Er, Tm, Yb and Lu were analysed by IC3R). The total REE contents of albitised psammites are 29.38 ppm (LA), 22.67 ppm (HA) and 15.54–16.62 ppm (complete albitisation).

The total REE content of amphibolite is present in the range of 139.32–160.85 ppm with the average of 150.09 ppm in two samples. A slight decrease of 20 ppm is present in depletion of the REE in albitised amphibolite. The REE patterns of amphibolite show no apparent changes between the albitised margin and the less albitised central sections (Figure 3.18D).

The REE pattern of biotite alteration shows a distinct depletion of the light REE content as well as the negative Eu anomaly but has no apparent effect on the heavy REE content (Figure 3.18A). The REE pattern of biotite alteration is strongly related to the REE pattern of albitisation of psammite through similar overall patterns but distinct variation of the overall content of REE, possibly reflecting the evolution of fluids from the albitisation to the biotite alteration system. However, Figure 3.18C shows that the REE pattern of biotite alteration is different from that of complete albitisation in psammopelite. The REE pattern has light REE enrichment against the patterns of albitisation in psammopelite. The REE patterns of breccias show negative Eu anomaly and overall flat trends of REE as distinct from the surrounding psammitic country rock (Figures 3.19). They have distinct enrichment of LREE and depletion of HREE comparing to metasediments. Biotite alteration resulted in a distinct increase of the LREE in pegmatite (Figure 3.18F).

The total REE content of pegmatite averages 78.12 ppm. Low level albitisation of pegmatite correlates with a distinct decrease of light REE content and to some extent also the heavy REE (Figure 3.18 E). The total REE contents of pegmatites are in the range of 6.89-155.73 ppm, representing the 4 types of pegmatites described above (Figure 3.19). Type (i) has a distinct negative Eu anomaly and elevated light REE contents (e.g. samples Pm017, BP032 and Ps035). Type (ii) albitised pegmatite has the value in the range of 1–10 of each element of nominated REE, depletion of light REE, a strong negative Eu and a distinct negative Ce anomaly in samples ABP022, Op031, PB034, AP041 and Ap042. The third type of pegmatite (iii) has an extreme depletion of REE and the most distinct negative Eu anomaly in addition to a positive Ce anomaly in sample Mp001, and the flat REE pattern was very close the chondrite norm or Bulk Earth. The pegmatite (iv) showed a clear negative Eu anomaly and a flat overall trend of REE in sample ABP025, however, the total REE content was clearly elevated (8 time chondrite). Albitisation has extreme depletion of LREE and remain the Eu negative anomaly.

The REE ratios are distinct in unalbitised and albitised rock, and are also variable among samples of a rock type (Table 5). LaN/YbN ratio in metasediments ranges from 2.23 to 23.84 but in albitised metasediments ranges from 0 to 5.73. The light REE are extremely depleted in albitised metasediments relative to unalbitised metasediments. The effect of depletion is similar to that in other albitised rock e.g. Am011 (amphibolite) has LaN/YbN of 32.54 compared to 25.91 of AbA012 (albitised amphibolite); and unalbitised pegmatite has LaN/YbN 20.40 in Ps035 compared to albitised pegmatite (Ps034) with a ratio of 3.34. The GdN/YbN ratio is 1.53-4.33 in unalbitised metasediments relative 0.58-1.28 in albitised metasediments.

Table 5 Rare earth element (REE) ratios and key relationships.

Sample no.	Rock types	LaN/YbN	LaN/SmN	GdN/YbN	CeN/YbN	CeN/SmN	EuN/YbN	Sum REE
L003	Psammite	15.72	1.88	3.77	13.82	1.66	2.39	559.83
UAP007	Psammite	23.84	1.98	4.33	21.23	1.77	3.11	529.74
PS008	Psammite	2.23	1.07	1.53	2.46	1.18	0.83	183.63
MPL016	Psammopelite	19.52	5.55	2.15	12.10	3.44	1.62	198.48
AB004	Albitised psammite	0.00	0.00	0.65	0.36	0.61	0.40	22.67
AB010	Albitised psammite	0.00	0.00	0.58	0.48	1.03	0.27	29.63
AB020	Albitised psammite	0.24	0.25	0.87	0.16	0.16	0.55	52.08
AB021	Albitised psammite	0.27	0.35	0.73	0.20	0.27	0.41	21.64
AB026	Albitised psammite	0.35	0.56	0.61	0.39	0.61	0.39	78.15
MAB014	Albitised psammopelite	2.23	1.40	1.28	1.53	0.96	0.76	16.26
HAB015	Complete albitisation	5.73	2.47	1.25	4.36	1.88	0.98	15.54
AB018	Albitised psammopelite	5.29	1.67	1.66	4.56	1.44	0.77	247.07
AB028	Albitised psammopelite	1.14	1.54	0.56	0.99	1.34	0.38	58.48
AB037	Albitised psammopelite	0.74	1.03	0.61	0.31	0.43	0.35	49.03
AB036	Albitised pelite	0.09	0.41	0.24	0.05	0.23	0.20	33.24
LCS029	Low alteration psammite	26.58	3.90	3.07	14.35	2.11	2.34	618.09
LMAB30	Mid-altered psammite	21.30	4.08	2.21	16.96	3.25	1.69	398.48
AB024	Altered psammopelite	0.46	0.56	0.80	0.27	0.33	0.53	66.42
AB027	Altered psammopelite	3.76	2.92	0.85	2.67	2.08	0.62	237.75
BAB039	Altered psammopelite	0.41	0.31	0.98	0.36	0.27	0.64	57.34
PSP038	Altered Pelite	28.75	4.61	2.59	19.71	3.16	2.21	351.21
B002	Breccias	0.11	0.16	0.86	0.68	0.99	0.48	65.73
PB005	Pipe breccias	0.57	0.54	1.01	0.90	0.86	0.46	181.5
BAB023	Breccia	4.59	2.28	1.40	4.12	2.05	0.87	440.5
PS040	Albitised breccia	1.00	0.69	1.00	1.12	0.78	0.74	100.04
BB033	Altered breccia	2.23	2.18	0.71	1.26	1.23	0.48	166.65
BI009	Biotite alteration	0.29	0.44	0.68	0.62	0.95	0.34	70.24
BI013	Biotite alteration	31.86	3.57	4.50	25.13	2.82	3.36	186.51
AM011	Amphibolite	32.54	4.09	3.61	25.09	3.16	3.16	160.85
ABA012	Albitised amphibolite	25.91	3.48	3.59	19.71	2.65	2.86	139.32
Mp001	Pegmatite	0.00	0.00	0.27	2.83	6.90	0.44	6.89
PM017	Pegmatite	8.02	2.64	1.56	6.31	2.08	1.26	153.27
OP031	Pegmatite	1.54	1.42	0.92	1.17	1.08	0.75	22.4
ABP022	Albitised pegmatite	1.76	1.19	0.96	1.34	0.90	0.78	36.7
ABP025	Albitised pegmatite	1.57	1.34	1.22	0.75	0.64	0.97	14.67
AP041	Albitised pegmatite	0.30	0.62	0.57	0.20	0.36	0.64	14.68
BP032	Altered pegmatite	4.37	1.87	1.23	3.68	1.58	0.77	258.89
PB034	Fine pegmatite	3.34	2.26	0.91	2.31	1.56	1.32	29.52
PS035	Coarse pegmatite	20.40	2.69	3.75	17.80	2.35	2.26	155.73
AP042	Altered pegmatite	0.89	0.62	1.09	0.92	0.67	0.75	88.41

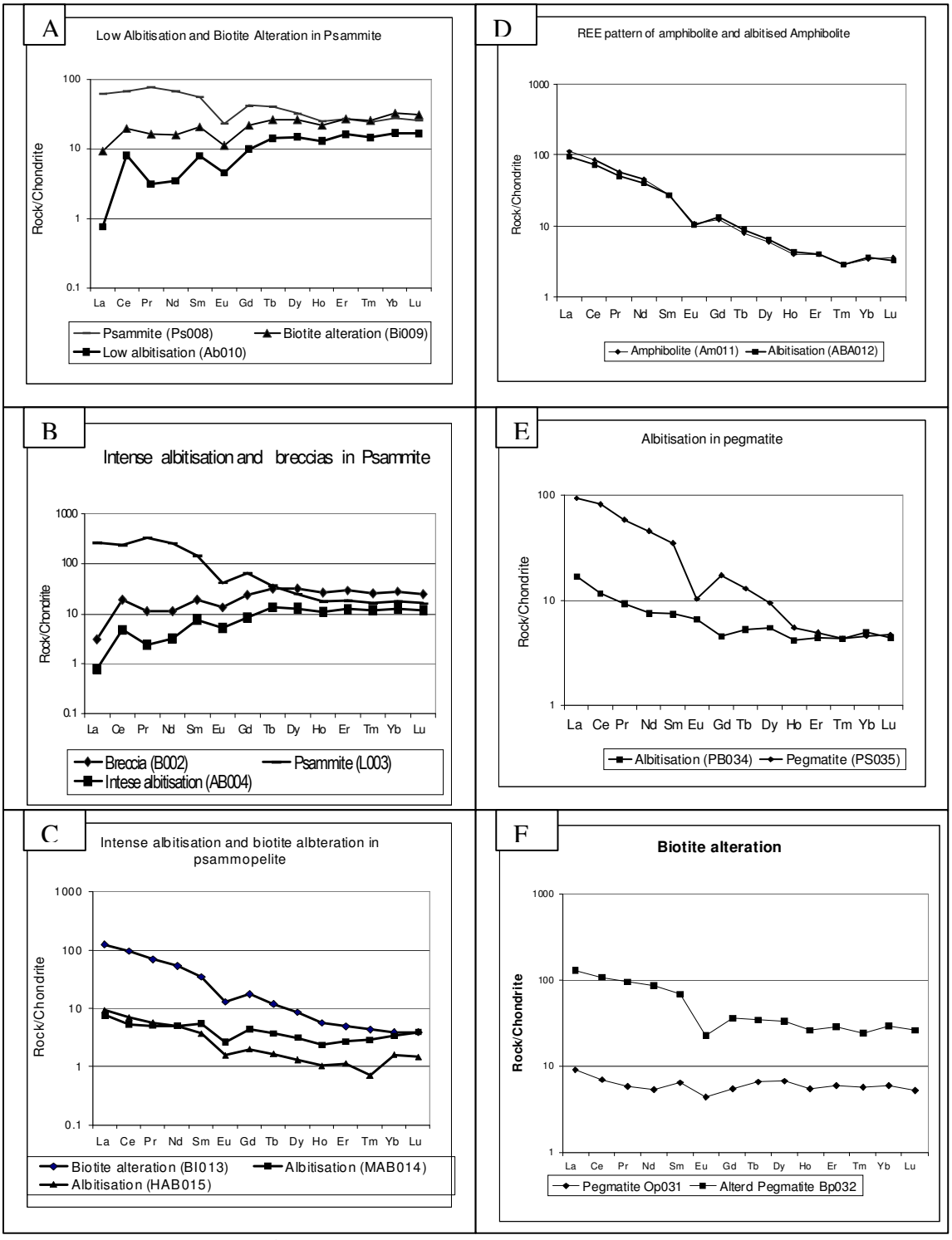

Figure 3.18 REE patterns of rock types: A. albitisation and biotite alteration in psammite; B. intense albitisation, breccia and unalbitised psammite; C. complete albitisation and biotite alteration in psammopelite; D. albitisation in pegmatite; E albitisation in amphibolite, F. biotite alteration in pegmatite.

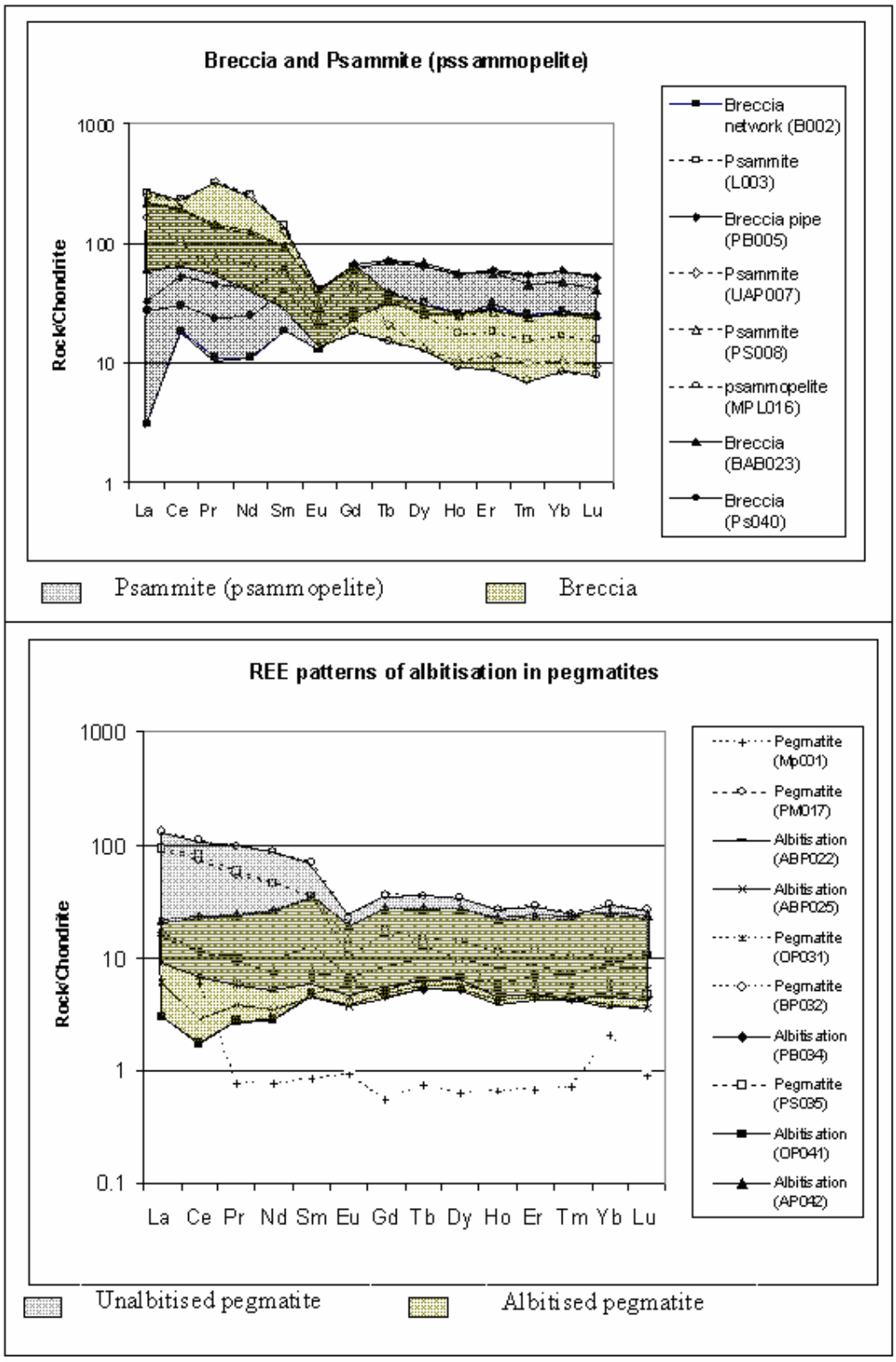

Figure 3.19 Chondrite normalised REE patterns, the top shows breccias and psammite/psammopelite. The bottom shows albitisation in pegmatite. The shades respectively represent breccias (yellow) and metasediments (grey) at the top; albitised (yellow) and unalbitised (grey) pegmatites at the bottom.

3.6 Microanalysis of Albitisation Mineralogy

3.6.1 Electron Microprobe

3.6.1.1 Plagioclase and K-feldspar

Six polished sections were selected as most representative samples of the three lithological groups for electron microprobe analyses (EMA). They were: psammite (Ps008) and albitised psammite (Ab010), amphibolite (Am011) and albitised amphibolite (AbA012), and pegmatite (Op031) and biotite altered pegmatite (Bp032). 14 elements (K, Na, Ca, Mg, Fe, Ti, Al, Si, P, Mn, Cr, Sr, Ba, F and O) were analysed in albite with the electron microprobe in these six sections. Analysed minerals were from: i) in psammite/albitised psammite; ii) in amphibolite/albitised amphibolite; iii) in pegmatite/altered pegmatite.

Figure 3.20 shows that in unalbitised psammite (Ps008) and albitised psammite (Ab010) all analysed plagioclase (15 and 13 mineral grains, respectively) is the end member–albite of composition $Ab_{96.5\text{-}98.4}$ in Ps008 and $Ab_{94.2\text{-}97.4}$ in Ab010. Only one in 13 points of feldspar analysis in sample Op031 revealed oligoclase. Figure 3.20 also shows that the confirmation of feldspar is albite composition in samples of metasediments.

Fifteen albite grains contain 7.38-12.13 wt% Na_2O in Ps008 of unalbitised psammite. EMA of twelve albite grains contain the average Na_2O 8.2 wt% in Ab010 of albitised psammite. This is resulted from very fine quartz within big albite crystals in albitised psammite.

Fluorine concentrations were measured in 15 grains and 12 grains of albite respectively in the primary (metamorphic) and secondary (albitised) phases by using the Electron Microprobe. Fluorine concentrations increase from the average 0.079 wt% F in the metamorphic phase in sample ps008 of psammite to the average 0.113 wt% F in the albitisation phase in sample Ab010 of albitised psammite.

In contrast, the analysed plagioclases in pegmatite (sample Op031) were $Ab_{83.4}Or_{2.1}An_{14.5}$ where 17 of 18 points of alkaline feldspar fell in two end member fields of albite and orthoclase (sample Bp032), $Ab_{93.4\text{-}98.0}$ in Op031 and $Ab_{90.0\text{-}97.4}$ in altered pegmatite (Bp032).

In amphibolite and albitised amphibolite ($Ab_{92.2–97.8}$ in Am011 and $Ab_{94.2\text{-}97.4}$ in AbA012) 7 points of plagioclase were determined to be albite. The remaining 4 points of plagioclase were identified to be oligoclase. Intermediate compositions between albite and orthoclase were rare: $Ab_{87}Or_{8.2}An_{4.0,}$ $Ab_{87.9}Or_{1.7}An_{10.4}$ and $Ab_{86.4}Or_{1.2}An_{12.4}$ were determined in unalbitised amphibolite Am011.

K-feldspars in pegmatites fall in the range of the $Or_{98.2\text{-}99.2}$ in sample OP031 and $Or_{93.9\text{-}98.8}$ to $Or_{86.1}Ab_{11.8}An_{2.1}$in sample (BP032, altered pegmatite) (Figure 3.20). 5 orthoclase grains in sample Op031 have < detection limit CaO but BaO in the range of 0.25-0.37 wt% BaO. 7 out of 11 orthoclase grains in sample Bp032 also contain 0.00 wt% CaO but rest four grains have 0.02-0.43 wt% CaO in Bp032. Eleven orthoclase grains have average 0.19 wt% BaO in the range of 0.08-0.30 wt%.

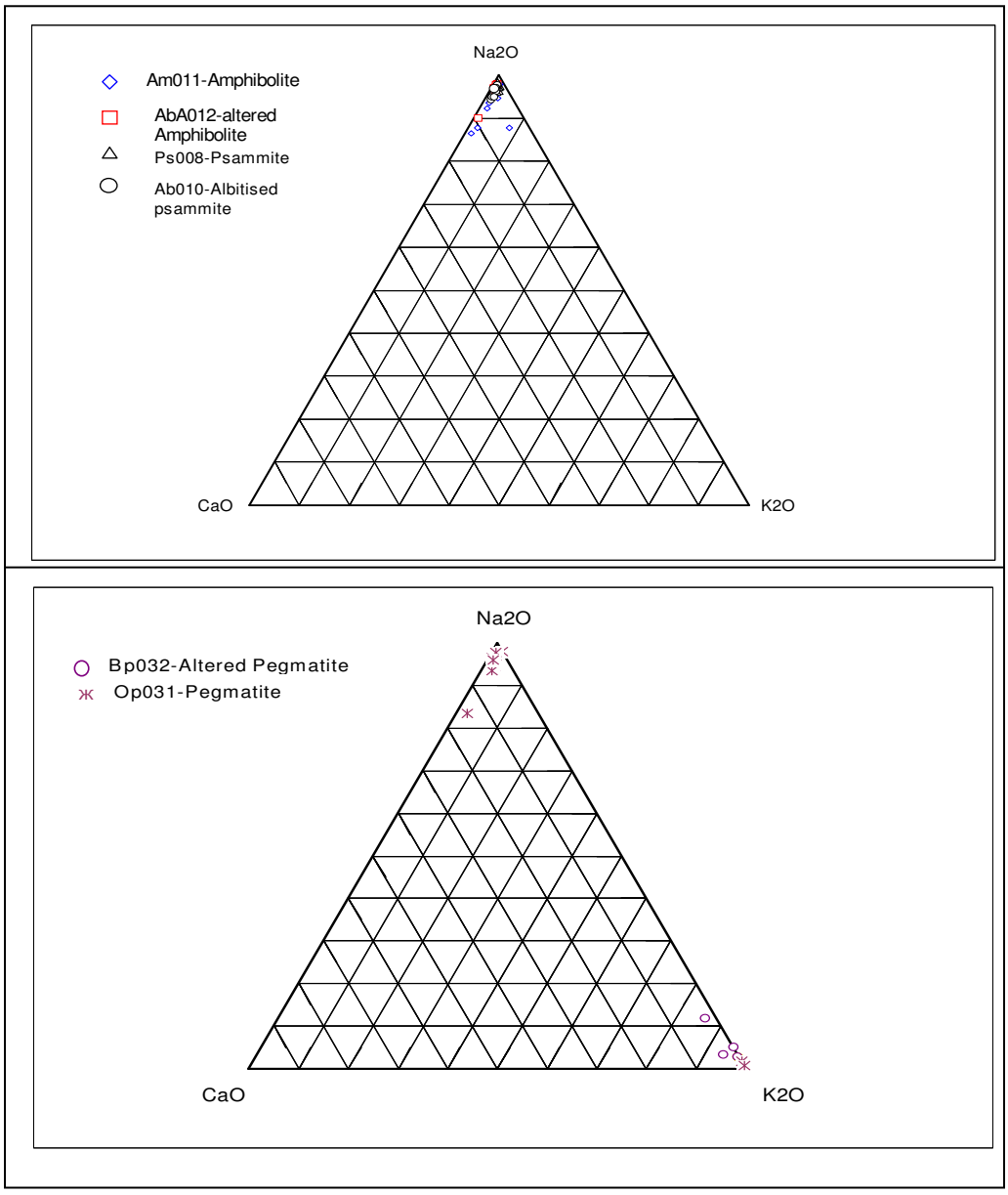

Figure 3.20 Na_2O-CaO-K_2O compositions of feldspars as determined by electron microprobe analysis; a) amphibolites and psammites, n=39; b) pegmatitic rocks, n=31.

3.6.1.2 Biotite and Muscovite

The composition of biotite of psammite is shown the Table 6. F content is at average 1.9 wt% in 14 biotite grains in psammite (sample Ps008).

The F average concentrations are 1.40 wt% in 6 biotite grains and 0.38 wt% in 6 muscovite grains of sample Ab010 (albitised psammite), 1.84 wt% in 6 biotite grains of sample Am011 (amphibolite) and 1.97 wt% in 5 biotite grains of sample AbA012 (albitised amphibolite).

The composition of two biotite grains (sample Op031 of pegmatite) is different from it in psammite. However, micas contains quite stable K_2O about 9 wt% in most rock types.

Table 6 The composition for biotite and amphibole

Sample	Psammite (Ps008)	Pegmatite (Op031)	Amphibolite (Am011)	Amphibolite (AbA012)
wt%	Biotite n=14	Biotite n=2	Al-Anthophyllite n=4	Ferri-Gedrite n=8
K_2O	8.74-9.74	8.52-8.96	0.09-0.18	0.06-0.23
Na_2O	0.10-0.94	0.16	0.11-0.13	0.11-0.13
CaO	0.00-0.02	0.00	0.0002-0.07	0.0002-0.06
MgO	14.98-17.23	1.93-1.94	18.18-19.31	18.00-19.04
Fe_2O_3	12.31-13.46	4.32-4.53	18.60-19.64	18.59-20.03
Al_2O_3	16.03-17.87	31.23-31.73	20.44-22.07	21.72-22.75
SiO_2	36.23-39.92	48.42-48.68	25.30-26.23	25.30-27.8
TiO_2	0.81-1.09	0.25-0.30	0.03-0.12	0.0002-0.10
MnO	0.04-0.21	0.00	0.26-0.36	0.31-0.43
P_2O_5%,	0-0.08	0.00	0.04-0.10	0.01-0.39
Cr_2O_3	0-0.04	0.00	0.00-0.01	0.00-0.05
BaO	0-0.15	0.04-0.07	0.003-0.16	0.0002-0.06
F	1.66-2.17	0.46-0.57	0.34-0.52	0.40-0.54

3.6.1.3 Magnetite

Two magnetite grains contain 0.75-0.85 wt% F, 0.10-0.20 wt% MnO and 94.06-95.66 wt% Fe_2O_3 (0.04-0.07 wt% SiO_2, 0-0.02 wt% TiO_2, 0.03-0.07 wt% Al_2O_3 wt%, 0-78 ppm Ba, 2-81 ppm Sr) in sample Am011 of amphibolite.

3.6.1.4 Amphibole (Anthophyllite/Ferri-Gedrite/Magnesiogedrite)

Amphibole is one of basic silicates in amphibolites as well as in some metasediments. Amphiboles are double-chain silicate minerals with the standard formula $A_{0-1}X_{2-3}Y_5[Si_8O_{22}](OH)_2$, where

A = Na, K, Ca, H_3O

X = Na, Ca, Mg, Fe but also Mn, Li

Y = Mg, Fe, Mn, Al, Ti

The amphiboles are classified in four groups depending on the X site.

1) Mg-Fe amphiboles
2) Sodic amphiboles
3) Ca amphiboles including
4) Sodic–calcic amphiboles (Shao 1978; Strauss 2003).

The chemical compositions of anthophyllite were quite consistent in both samples, Am011 and AbA012 (Table6). In sample Am011, the variation of anthophyllite composition was shown in table 6 for the range of elements (SiO_2, Al_2O_3, Na_2O, MgO, Fe_2O_3, K_2O, CaO, TiO_2, MnO, Cr_2O_3, P_2O_5 and F and BaO (points Am011-4-2, 5-2, 6-2 and 7-4). The chemical formula of anthophyllite may be written out as $Fe_5Mg_4Al_4Si_4O_{12}(F_{0.1})(OH)x$ by using the proportions of atomic numbers

($Fe_{15}Mg_{11.6}Al_{11.5}$ $Si_{12}O_{36}F_{0.3}$)(OH)x. From the standard formula, Anthophyllite may be classified as Al-anthophyllite.

In sample AbA012, the compositions of 9 points of Al-Anthophyllite were also shown in Table 6 for the range of SiO_2, Al_2O_3, Na_2O, MgO, Fe_2O_3, K_2O, CaO, TiO_2,MnO, Cr_2O_3,P_2O_5, F and BaO (points AbA012-1-3, 3-1, 6-3, 6-4, 6-6, 6-7, 6-8 and 6-20). The chemical formula $(Mg, Fe)_7[Si_4O_{11}]_2(OH)_2$ of Al-anthophyllite was written in $Fe_5Mg_4Al_4Si_4O_{12}F_{0.1}$(OH)x simply by using the proportions of atomic numbers ($Fe_{15}Mg_{11.2}Al_{11.7}Si_{12}O_{36}F_{0.3}$). Al-anthophyllite contains 0.17-0.42 wt% of Na_2O + K_2O + CaO. Thus, the amphibole may approximate to Al-Anthophyllite in chemical standard formula $A_{0-1}X_{2-3}Y_5[Si_8O_{22}](OH)_2$ - $Na_{0.1}Mg_3Fe_5[Si_8O_{22}](OH)_2$. The hydroxyl ions may be replaced partly by F as well as Cl. Figure 3.21 shows that very stable compositions in the ternary plots of anthophyllite in 13 points (samples Am011 and AbA012).

From web Mindat.org (2008-06-19), the Al-anthophyllite is a Magnesiogedrite in both Strunz and Dana Classes for Anthophyllite classification. A classification of amphiboles (AMPH-CLASSS: MS Excel spreadsheet) is based on the 1997 recommendations of the International Mineralogical Association (Esawi 2004). Following this, the Al-Anthophyllite is a Ferri-Gedrite.

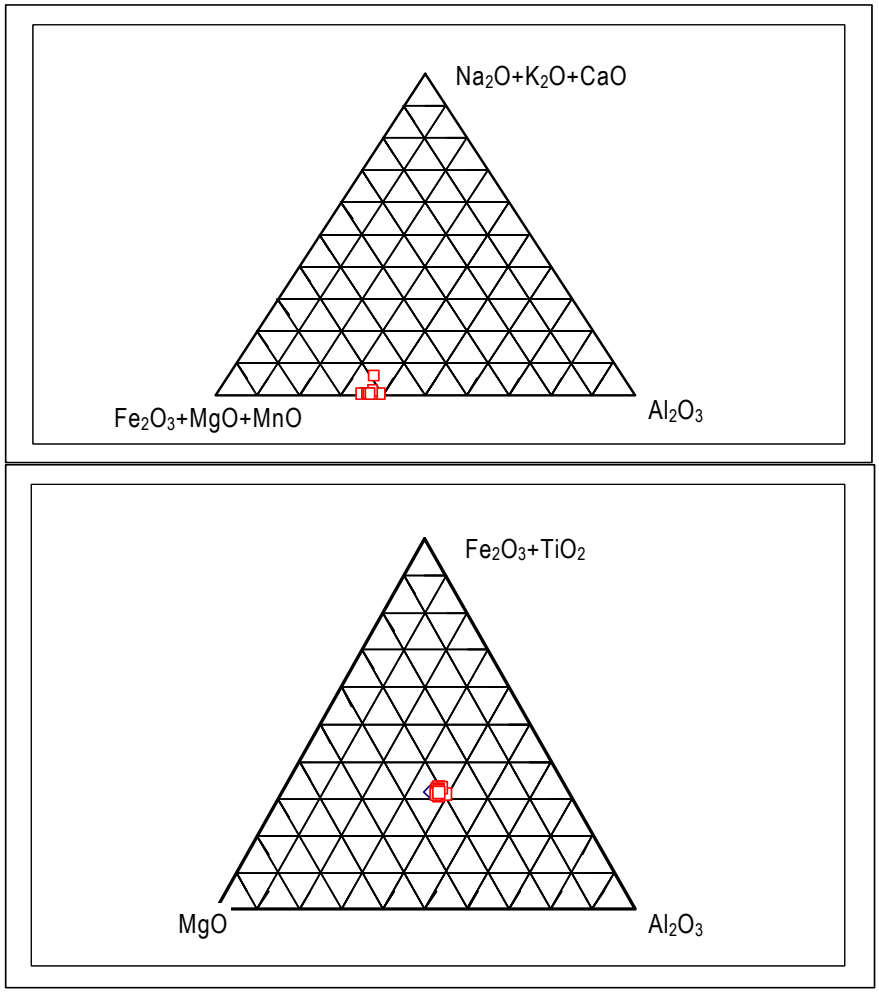

Figure 3.21 Ternary plots for Al-Anthophyllite (Ferri-gedrite) in amphibolites.
Notes: 1. Na_2O+K_2O+CaO are at A-site. $Fe_2O_3+MgO+MnO$ are at X-site. 2. Al-Anthophyllite/Ferri-gedrite ternary plots in 15 points of amphibole in Am011 and AbA012.

3.6.1.5 Accessory Minerals

Accessory minerals were garnet, tourmaline, ilmenite, rutile, hematite, pyrite, barite, zircon, titanate, apatite and possible fluorite (see chapter 3.5.1). The crystals of fluorapatite were measured by Electron Microprobe. The chemical compositions of fluorapatite consist of 54.72-56.50 wt% CaO, 42.88-43.73 wt% P_2O_5, 5.11–5.33 wt% F, 0.16-0.17 wt% Na_2O, 0.16-0.18 wt% MnO, and 0.12-0.24 wt% Fe_2O_3 in points, Am011-5-3 and AbA012-1-2. Apatite contains 54.58 wt% CaO, 41.36 wt% P_2O_5, 1.23 wt% F, 2.27 wt% Cl and 0.56 wt% H_2O in $Ca_5 (PO_4)_3F$ OH (Shao 1978). The chemical formula can be written as $Ca_5 (PO_4)_3F$ – fluorapatite by proportion of atomic number. The specific apatite-F are characterised by rich F (5.23/1.23) involved 0.16-0.17 wt% Na_2O in both centre of amphibolite and albitisation edge.

3.6.2 Laser-Ablation-Inductively Coupled Plasma Mass Spectrometry (LAICPMS) analysis

LAICPMS analysis was used to determine the trace element composition of minerals based on the results of Electron Microprobe Analysis (see Chapter 2.4). Six polished thin sections of samples (Ps008, Ab010, Am011, AbA012, Op031 and Bp032) were selected to represent the respective primary and albitised/altered rock types. Unfortunately, the albitised amphibolite (AbA012) has a little less Na than the low albitisation amphibolite (Am010); the unaltered pegmatite (Op031) has higher Na and K concentration than biotite alteration of pegmatite (Bp032). Only high Fe concentration in Bp032 can reflect the biotite alteration compared to unaltered pegmatite (Op031). Further analysis of trace and rare earth element variation in albitised/altered rocks were carried out by using the Laser Ablation ICP MS probe at the University of Adelaide.

Minerals analysed are plagioclase (albite), alkaline feldspar (orthoclase), amphibole (Al-anthophyllite/Ferri-gedrite/Magnesiogedrite), micas (biotite and muscovite) and selected accessories. The individual mineral grains were analysed by electron microprobe for major elements to allow accurate calibration of LAICPMS analysis. Analyses were carried out along the following routine steps:

1) location of the points for analysis of the minerals,
2) selecting the transport rate of ions and package of interesting elements,
3) analysis of the nist 612 in 3-4 spots for calibration and selection 1 standard element,
4) instrument 1 or 2 standard element for individual minerals in sample,
5) testing of analyzing the glass of the sample slides,
6) determination of background of signals per analysis, and
7) selections of laser energy level and ablation spot size setting.

The locations were selected to be at least 5 times of the diameter of the ablated spots. For example, 30 μm ablation spot size needed a 150 μm mineral grain to avoid fracturing of the mineral grain during the ablation processes. The thicknesses of polished sections were approximately 100 μm and thus in excess of the possible ablation penetration depth which was set at 10 μm to avoid ablating the underlying glass slide. Sites for analyses were selected with care to not contain contaminants such as small mineral inclusions. Dust and other contaminants were removed from the section surface with analytical grade alcohol. The calibration standard used was the nist 612 (Durrant 1999) calibration procedures followed recommendations from Angus in Adelaide microscopy (Durrant 1999; Trotter & Eggins 2006).

Analytical data from 156 ablation points were attained in five minerals, albite, K-feldspar, plagioclase, amphibole and biotite. 75 data sets were removed from the data sets due to uncertainties of analytical accuracy. Analytical data of the remaining 71 points were considered reliable.

The quality of data depends on the signals of each element in parson distribution intervals. Actually, Na is a good element for albite for decision of the intervals of signals. Change of signal interval means data automatically changes the optimized intervals. The signals of each element are reliable, because:

1) the element signals have an un-saturation peak; two or more peaks of signals should be given up,
2) location changes result in un-reliable analysis, (wrong minerals and wrong mineral grain),
3) major element saturation results in trace element below detection limits;
4) sample standard element Al can not cover all analysis elements in some cases, Fe is not a good sample standard element,
5) the interval of signal review is too narrow to analyses;
6) 35-45 second intervals may be common good analyses.

The data are presented in four forms: element concentrations in ppm in minimum detect limits (MDL) filtered, 1 sigma error, minimum detection limits <99% confidence and element concentrations normalized to chondrite, this data set is automatically provided by the application software "GLITTER!" (Jackson 2001). For example, for albite, the ratio of Na/K and Na/Ca were 10:1 to 100:1 roughly, the ratio of Na_2O/Al_2O_3 was about 1:2. For amphibole, the ratio of Al/Fe was about 21:16. For biotite, the ratio of K/Fe was 9:12. These ratios were known from electron microprobe analyses carried out previously.

Good analytical data of LAICPMS should be consistent with the known ratios from EMA in each of the points of analysis. Values below the detection limit of the ICPMS instrument could be the result of bad calculation so that more than three REE elements analysed were systematically unreliable and were not processed in the REE patterns. Bad signal reviews resulted in unreliable data for single major elements but calibrations normally remain the correct shapes/relationships of patterns. All sets of data can be optimized by a known concentration of original records in calculations in Excel 2003 based on the nist 612 without changes of the signal review. Change of the signal review can optimize data calculation in Adelaide Microscopy. 1 Sigma error (standard deviation) value indicates the degree of accuracy of data for each element. The element concentration is reliable in the range of <0.1 of (1 Sigma error)/concentration ratio.

3.6.2.1 Unalbitised Psammite

A total of thirteen grains of albite, plagioclase and biotite in sample Ps008 of unalbitised psammite, were analysed for their REE contents. Total REE content was in the range of 51.33 to 236.36 ppm for albite, 13.71 ppm for plagioclase and 1.88 to 19 ppm for biotite. The chondrite normalised REE patterns demonstrate that albite has distinct negative Eu and Ce anomalies (5 analyses) (Figure 3.22). The REE patterns of plagioclase similarly have a negative Eu anomaly and show a distinct enrichment of the light REE. REE patterns of biotite have a positive Ce anomaly but only an indistinct Eu anomalism and a slight enrichment of the heavier elements (Figure 3.22).

3.6.2.2 Albitised Psammite

A total of twelve grains of albite, amphibole and biotite in sample Ab010 of albitised psammite were analysed for their REE contents (see appendix C-2). Nine albite grains

display a negative Eu anomaly and in some cases a positive Ce anomaly, overall REE contents are variable (Figure 3.22). The REE patterns of amphibole show a distinct increase from the light to the heavy elements. Total REE contents of biotite fall in two ranges, 400.12-472.42 ppm and low value 2.50 ppm, possibly implying two generations of biotite, however, their overall chondrite normalised patterns are similar with a gentle decrease from the light to the heavy elements (Figure 3.22). A slight negative Eu anomaly is present in one of three biotite grains. The REE patterns of albite and biotite were changed during albitisation completely.

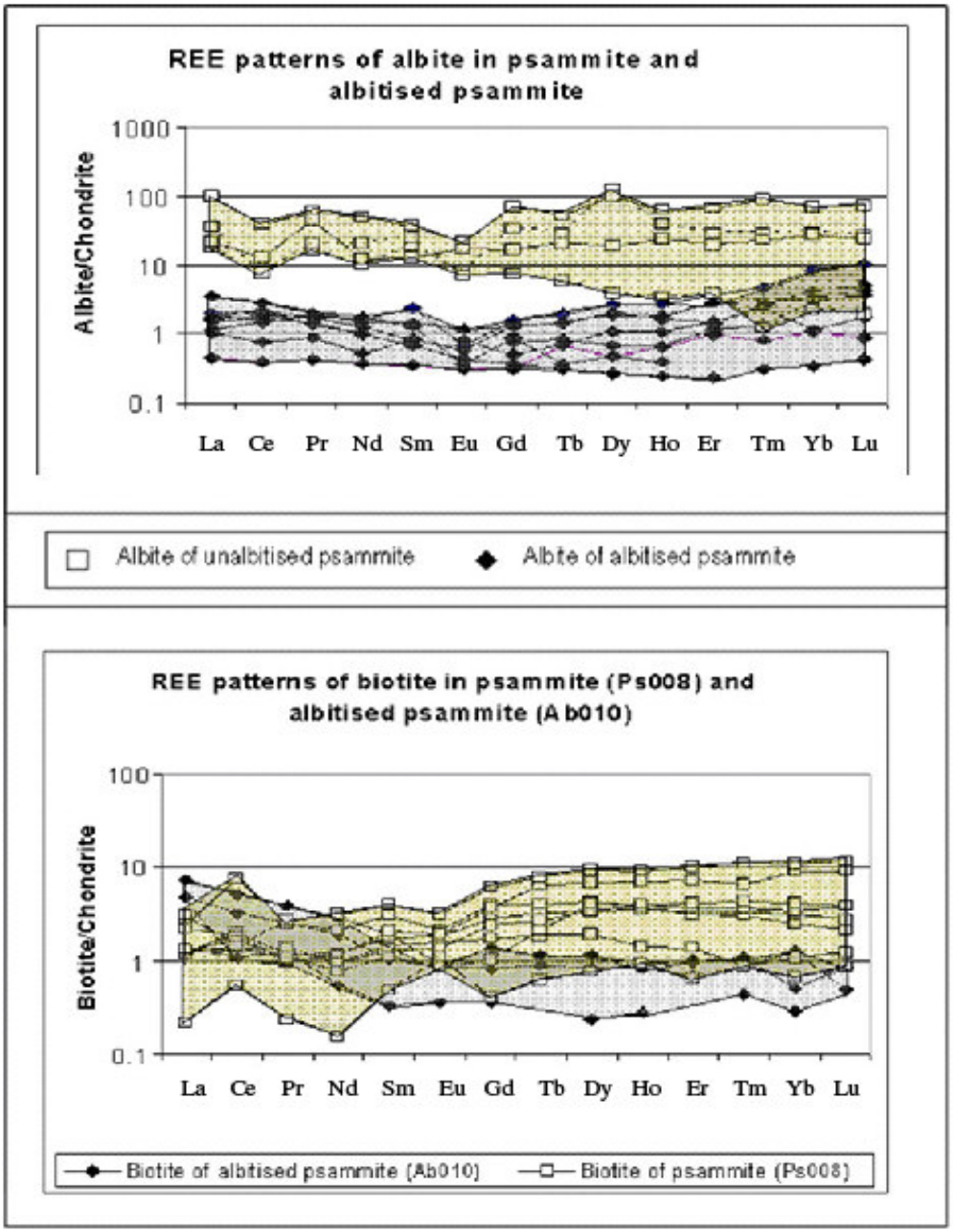

Figure 3.22 REE patterns of minerals in unalbitised (sample Ps008) and albitised psammite (Ab010). The shades represent unalbitised (yellow) and albitised (grey) psammite. The top is for albite and the bottom is for biotite.

3.6.2.3 Low albitisation Amphibolite

Ten grain total of albite, amphibole (Anthophyllite) and biotite were analysed in the least albitised amphibolite from the centre of the amphibolite outcrop (sample Am011, Figure 3.23). Four albite analyses revealed a distinct enrichment of LREE over HREE as well as a negative Eu anomaly.

The REE pattern of biotite and amphiboles follow trend very similar to the albite with an enrichment of light over heavy elements and a slight Eu anomaly.

3.6.2.4 Albitised Amphibolite

Seven grain total of albite and amphibole were analysed in albitised amphibolite from the margin of the outcrop (sample AbA012, Figure 3.23). The REE patterns of albite were clearly presented at the average sum 25.18 in range of sum 15.73-30.12 of nominated value to chondrite. Three albite grains revealed distinct decrease from LREE to HREE and a negative Eu anomaly. REE patterns of amphiboles were present at a total REE content at the average of 31.91 in the range of 15.91-43.05 of nominated value to chondrite. Several analyses revealed a slight to distinct Eu anomaly and in two cases a negative Ce anomaly.

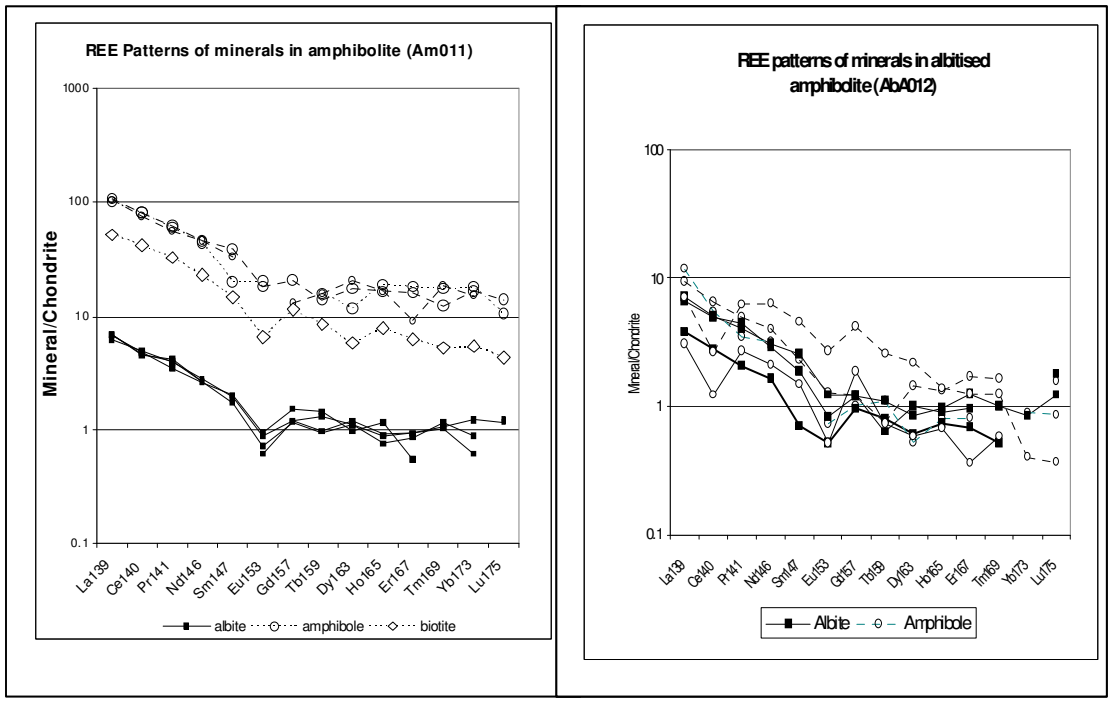

Figure 3.23 REE patterns of minerals in amphibolite (Am011) and altered/albitised amphibolite (AbA012).

3.6.2.5 Unaltered Pegmatites

Nineteen grains of albite, plagioclase (rather than albite), K-feldspar and biotite were analysed in the pegmatite sample Op031 (Figure 3.24). Figure 3.24 shows the REE patterns of six albite grains has a distinct enrichment of LREE and a well expressed negative Eu anomaly. A grain of albite contains some enrichment of LREE but unapparent Eu anomaly in low value range of 0.29–2.04 of albite/chondrite. The REE

patterns of three plagioclase grains show the positive light REE, negative Eu anomaly and positive Tm anomaly in the normal range of 0.99–103.1 nominated value in pegmatite. The patterns show the main high value group for two grains and the main low value group for one grain. Figure 3.24 shows the REE patterns of nine K-feldspar grains with the positive light REE, negative Eu anomaly and positive Tm anomaly in both, the main low REE nominated-value group and the high value group. The REE pattern of one biotite grain shows the Eu negative anomaly in the very narrow range of nominated value 4.8–12.24. The REE patterns of minerals may imply that the two main phases existed for plagioclase and K-feldspar. The REE patterns of albite are present in low main phases but the lower minor phase existed. The very intensive albitisation would partly exist in a possible minor process.

3.6.2.6 Biotite Altered Pegmatite

The optimum data of minerals were believed to be reliable (see chapter 2.4). Eight grains of albite, plagioclase, K-feldspar and biotite in sample Bp032 of altered (biotite alteration) pegmatite, were analysed to determine their REE contents (Figure 3.24). The REE pattern of one albite grain shows the negative Eu anomaly and an enrichment of heavy over light REE. The REE patterns of K-feldspar, plagioclase and biotite grains show enrichment in light REE and depletion in heavy REE. All analyses show the enrichment of the LREE over the HREE except albite (Figure 3.24). The REE patterns of one orthoclase grain has low sum of the REE and a positive Eu anomaly. Thus, K alteration has positive Eu anomaly compared to albitisation during biotite alteration of pegmatite (see Chapter 3.5.2 and Appendix-C).

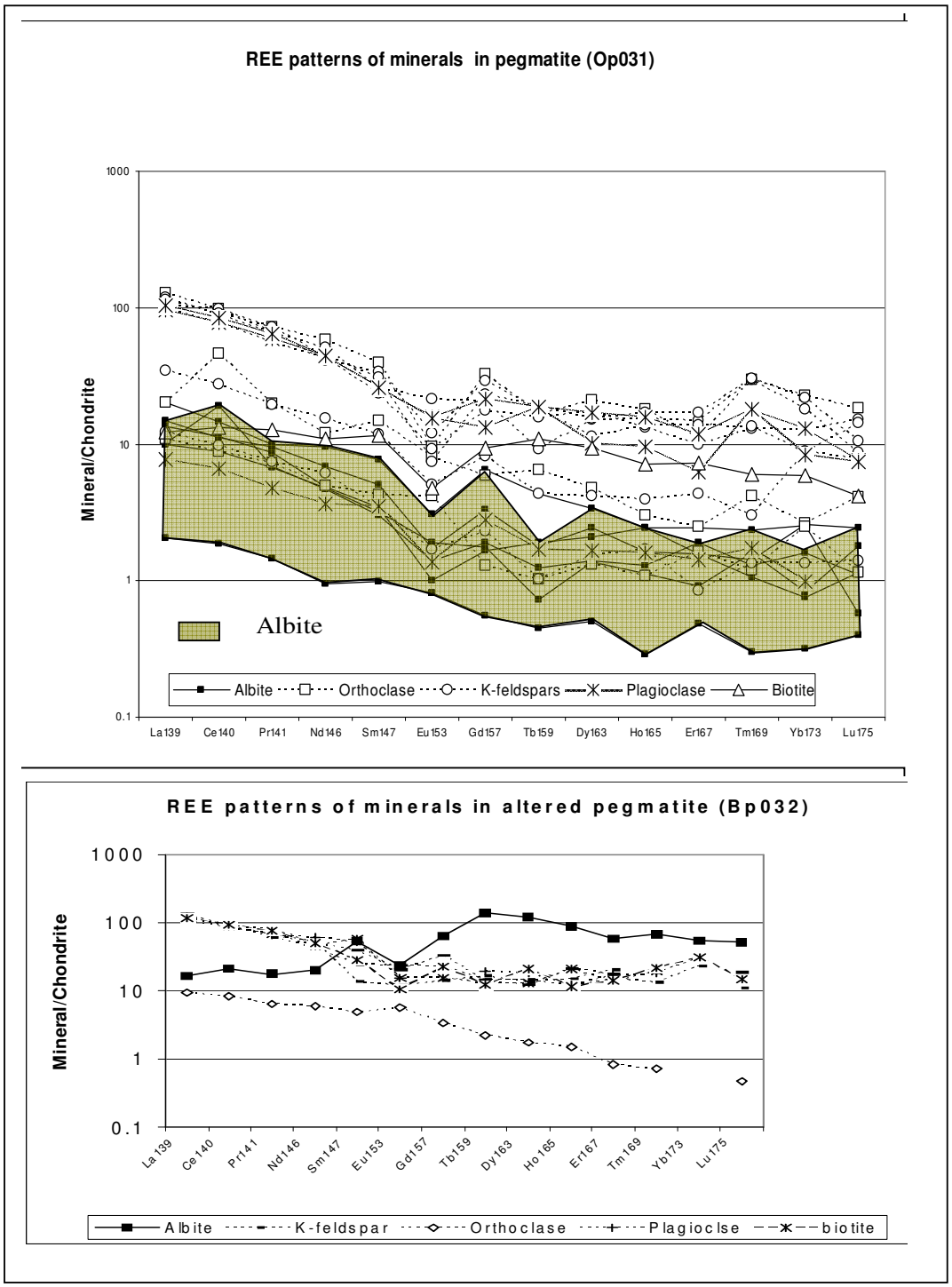

Figure 3.24 REE patterns of minerals in pegmatite and altered pegmatite.

3.6.2.7 REE contents of individual mineral phases

The REE ratios of LaN/YbN of albite show great variations of the range from average 1.9 (albitised psammite) to 21.07 (albitised amphibolite) in sample grains in all rock types (Table 7) with minimum 0.3 (altered pegmatite) to maximum 48.71 (albitised amphibolite), see appendix C. LaN/YbN ratios of albite show more stable range of 0.31-4.58 in albitised psammite than of 0.57-16.47 (average 4.81) in psammite. CeN/SmN ratios of albite are relative small variable in the range of average 0.68 (psammite) to 3.07 (pegmatite) with GdN/YbN in the range of average 0.83 (albitised psammite) to 5.03 (albitised amphibolite). The heavy REE of albite has the stronger fractionation than the light REE in all rock types. The REE ratios of biotite are quite stable in all rock types compared to feldspar (albite, K-feldspar and plagioclase). For example, biotite of psammite has average 0.5 LaN/YbN, 0.84 LaN/SmN, 0.84 GdN/YbN, 0.87 CeN/YbN, 1.18 CeN/SmN and 0.70 EuN/YbN ratios. However, distinguishable is that biotite of albitised psammite has average 7.59 LaN/YbN, 4.17 LaN/SmN, 1.51 GdN/YbN, 5.55 CeN/YbN, 3.06 CeN/SmN, and 1.26 EuN/YbN ratios. The great fractionations of light REE change gradually to the slight fractionation of the heavy REE in biotite of albitised psammite. That means the secondary biotite in albitised psammite may replace the primary biotite in psammite mostly during albitisation.

Table 7 Average of chondrite normalised REE ratios for individual mineral phases.

	LaN/YbN	LaN/SmN	GdN/YbN	CeN/YbN	CeN/SmN	EuN/YbN
Psammite(Ps008)						
Minerals						
Albite	4.81	1.67	1.48	1.17	0.68	1.09
Plagioclase	7.71	3.94	1.38	6.12	3.13	1.06
Biotite	0.50	0.84	0.84	0.87	1.18	0.70
Albitised Psammite (Ab010)						
Albite	1.90	1.85	0.83	1.88	1.70	0.54
Biotite	7.59	4.17	1.51	5.55	3.06	1.26
Amphibole	0.06	0.13	0.32	0.09	0.19	0.44
Amphibolite (Am011)						
Albite	7.98	3.66	1.43	5.66	2.49	0.87
Al-Anthophyllite	6.36	2.98	1.19	4.72	3.38	0.81
Biotite	9.58	3.54	2.13	7.69	2.84	1.21
Albitised Amphibolite AbA012						
Albite	21.07	3.89	5.03	14.91	2.73	2.82
Plagioclase	42.90	3.57	10.73	28.45	2.35	3.68
Amphibolite	37.42	19.10	13.85	19.94	9.00	6.80
Pegmatite (Op031)						
Albite	10.46	3.00	2.60	9.48	3.07	1.81
K-feldspar	6.93	3.25	1.53	6.90	2.82	1.18
Plagioclase	9.20	3.30	2.03	7.61	2.72	1.48
Biotite	2.06	1.06	1.57	2.20	1.14	0.81
Altered Pegmatite Bp032						
Albite	4.61	1.98	1.10	3.34	1.47	2.53
K-feldspar	5.06	4.77	0.99	3.76	3.82	1.01
Plagioclase	3.80	2.32	0.00	2.79	1.50	0.49
Biotite	3.81	4.13	0.74	3.03	2.37	0.35

3.6.2.8 Trace elements of minerals

The concentrations of trace elements were also analysed by LAICPMS. All optimum data were reliable by studying the methods (see Chapter 2.4 and Appendix C). Extreme depletion was determined for Co, Ni, Cu, Zn, Ba, Pb and U in albite in albitised psammite (Ab010) compared to unalbitised psammite (Ps008), Ga and Sr concentrations are variable or non systematic (see Figures 3.25 and 3.26). The similar element depletion was also clearly present in albite in unalbitised amphibolite (Am011) and albitised amphibolite (AbA012) in Figure 3.27. Albite has consistent depletion of concentrations of Co, Ni, Cu, Zr, Sr, Pb and U in unaltered pegmatite (Op031) but uncertainty was present in biotite alteration of pegmatite (Bp032) in Figure 3.28.

Albite in albitised psammite has lower concentrations of Co, Ni, Cu, Zn, Ba, Pb and U (e.g.198.94 ppm Cu, 0-1.19 ppm Co and 0-1.89 ppm Ni) than albite in unalbitised psammite has (634 ppm Cu, 3.54-91.12 ppm Co, 6.16-208.32 ppm Ni) (Figures 3.25 and 3.26). Plagioclase and biotite in albitised psammite have slight variation of concentrations of Ba and Sr compare to these in unalbitised psammite. Variation of Co, Ni, Cu, Zn, Pb and U in plagioclase and biotite is similar to these in albite from unalbitised to albitised psammite. Au concentration is 0 - <0.10 ppm in albite in albitised psammite and 0.063 ppm (one grain) in albite in unalbitised psammite. Albitisation has extremely depleted the concentration of Co, Ni, Cu, Zn, Ba, Pb and U, even Sr and Au of minerals completely in psammite (metasediments) with the exception of uncertain Ga. The extreme depletion is derived from main albite and minor biotite between metamorphism and albitisation phases.

Albite in amphibolite has low concentrations of Co (<0.30-<0.32 ppm), Ni (<0.58-<0.98 ppm) and Cu 3.96 – 4.19 ppm) similar to Co <0.24 - <0.49 ppm, Ni <0.48 - <1.02 ppm and Cu <0.97 - 5.01 ppm in albitised amphibolite (AbA012) (Figure 3.27). So are the rest elements in albite. The least albitised amphibole in Am011 has the higher concentration of U (6.96-10.19 ppm) than them (0.12-0.90 ppm) in albitised amphibolite (AbA012). U, Zn, Cu, Sr, Zr, Sr, Ba and Pb of amphibole are depleted but Ni and Co are enriched, uncertain is Ga. Albitisation has changed the concentration of trace elements although the changes are very slight in Ga, Sr, Zr and Ba in minerals between the least albitised and albitised amphibolite.

Albite has highly variable concentrations of trace elements in biotite alteration of pegmatite, and albite maintains the concentrations of Co, Ni and Cu but increase of Ga, Sr, Ba and Pb (Bp032 match with Op031) (Figure 3.28). Orthoclase has high concentrations of trace elements in unaltered pegmatite (Op031) but it has very low concentrations of trace elements in biotite alteration of pegmatite (Bp032). Biotite has less variable concentration of trace elements in Bp032 than that in Op031. Au concentrations are below the detection limitation (0.019 -1.42 ppm and 0.058-4.17 ppm) in all minerals in unaltered pegmatite (Sample Op031) and in biotite alteration of pegmatite (Bp032). These changes are related to the re-distribution of trace elements of minerals between unaltered and biotite altered pegmatite compared to albitisation.

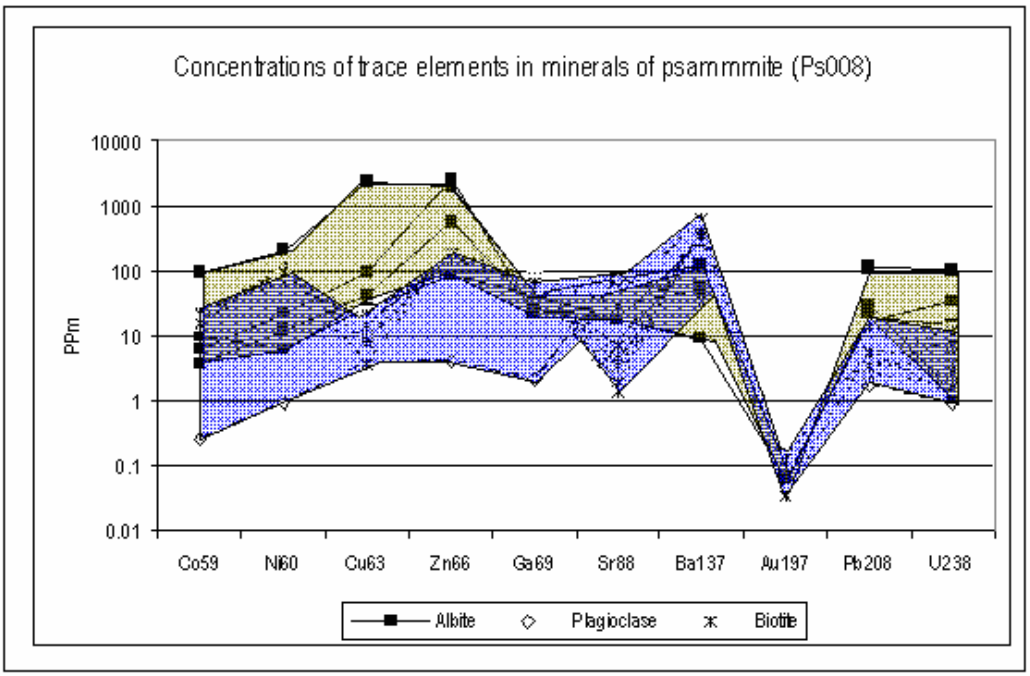

Figure 3.25 Concentrations of trace elements of minerals in unalbitised psammite (Ps008).
Notes: 13 grains of minerals were analysed by LAICPMS in psammite (Ps008) for Co, Ni, Cu, Zn, Ga, Sr, Ba, Au, Pb and U concentrations. These grains are four albite, one plagioclase and eight biotite grains which were calculated respectively by Na, Al and K from preparation of results of EMA in the same points/grains. Albite has high concentrations of Sr, Cu, Pb, Zn and U. Plagioclase has the low concentrations of the ten elements. Biotite has low U, Pb, Sr, Zn, Cu and Au but high Ba, Ni, Co and Ga compared to albite (see appendix C-2 for details).

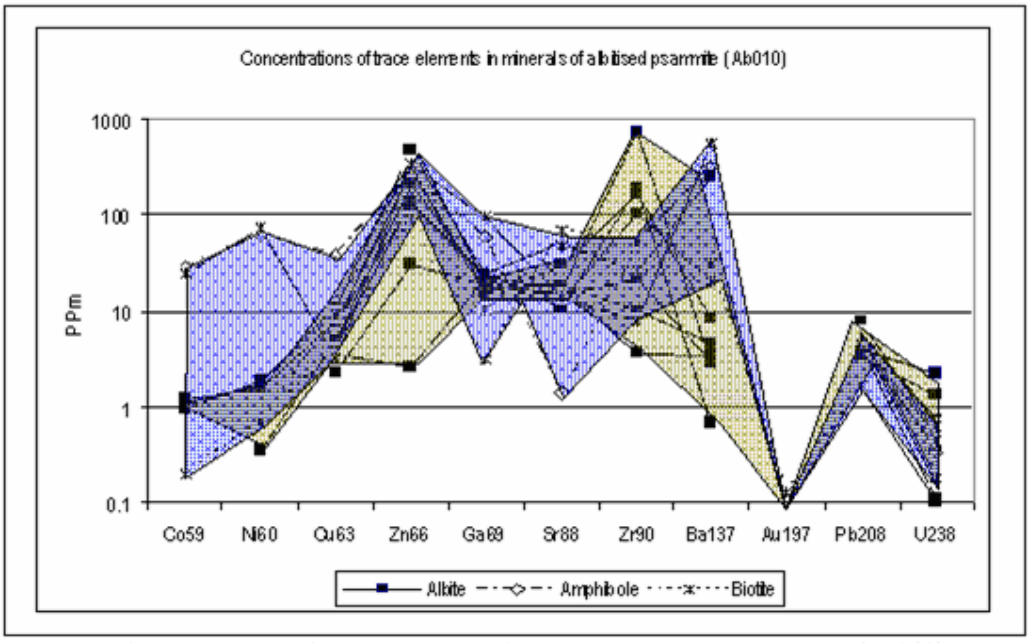

Figure 3.26 Concentrations of trace elements of minerals in Albitised psammite (Ab010).
Notes: Twelve grains of minerals of albitised psammite were analysed by LAICPMS in Adelaide microscopy for trace elements.

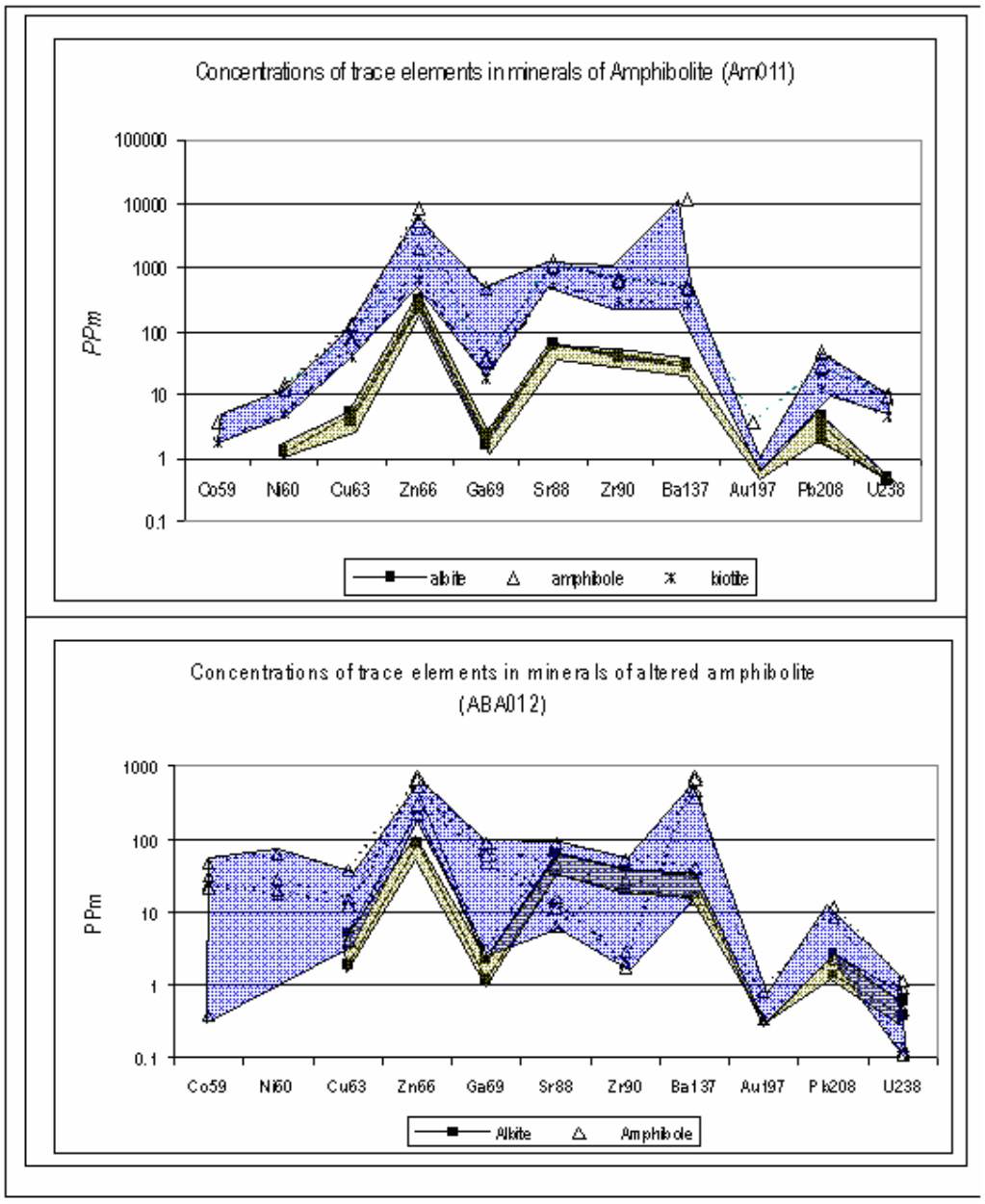

Figure 3.27 Concentrations of trace elements of minerals in amphibolite (Am011) and albitised amphibolite (AbA012).

Notes: 1.Trace elements of 17 mineral grains were analysed respectively in amphibolite (10 grains) and albitised amphibolite (7 grains) by LAICPMS in Adelaide Microscopy.

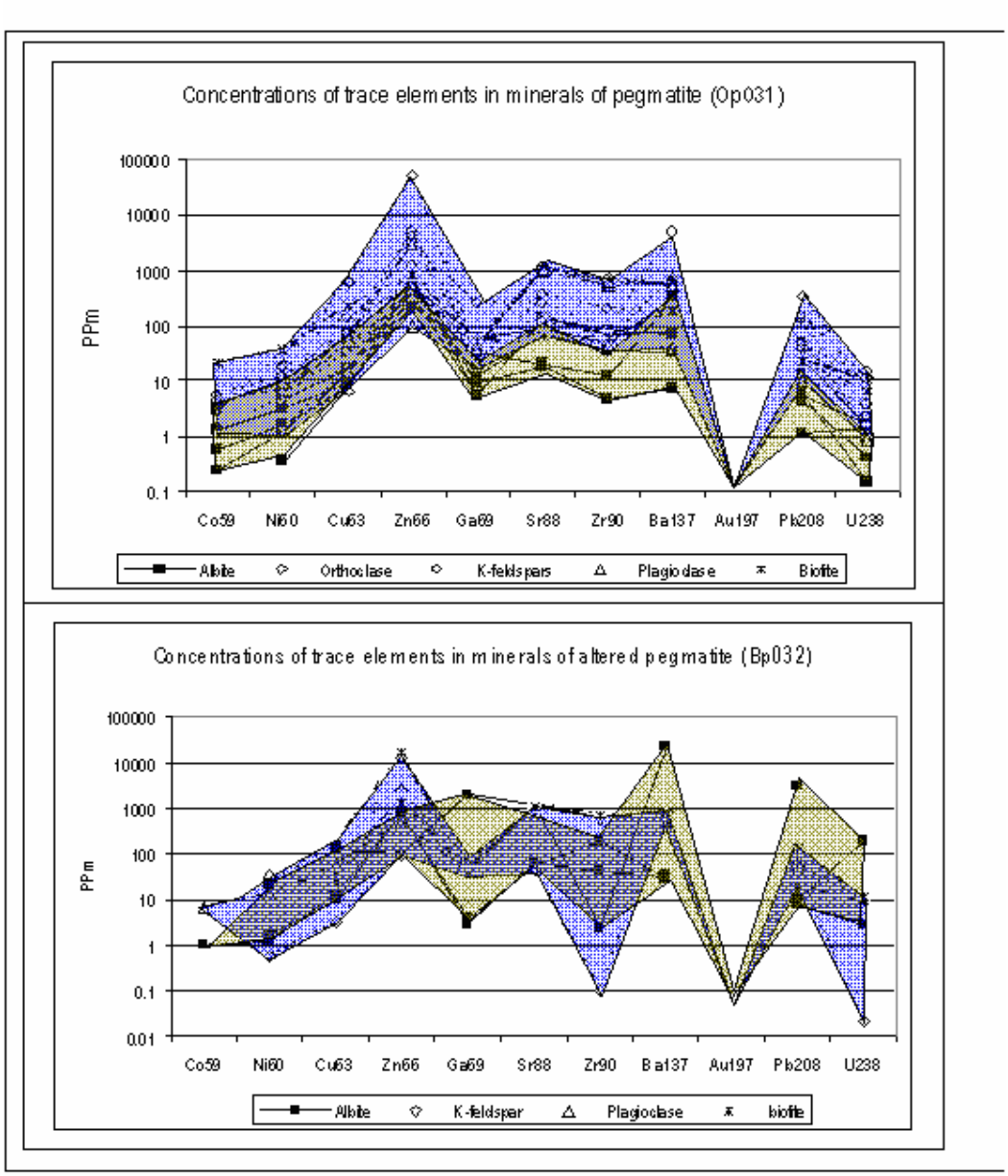

Figure 3.28 Concentrations of trace elements of minerals in pegmatite (Op031) and biotite alteration of pegmatite (Bp032).
Notes: Twenty nine mineral grains were analysed respectively in pegmatite (19 grains) and biotite alteration of pegmatite (10 grains) by LAICPMS in Adelaide Microscopy.

3.7 Results of the mass balance estimates

The immobile elements were selected in each sample group respectively (see chapter 2.5). From original dot draw a straight line at a best fit to have the most immobile elements as a group. Then, using the immobile elements calculated the Iscons slopes respectively.

ρ value is 2.74 at minimum and 3.75 at maximum in 9 samples of granites from the three garnet-chlorite shear zones, within the Walter-Outalpa shear zone (Clark et al. 2006). ρ value (psammite) is 2.74 at maximum and (albitised psammopelite) 2.6 at minimum in ten samples of lithologies in the Telechie Valley (Clark et al. 2005). It means ρ^A/ρ^O ratios/slopes are in range of 0.69 (2.6/3.75) to 1.44 (3.75/2.6). The calculation results are 0.73 to 0.93 well in the range as above for albitisation.

The albite ρ value is about 2.62 and the biotite has an average density of 3.09. The density of main mineral biotite is higher than albite density; and the Fe, Mg and Ba heavy minerals involved in biotite alteration. The calculation result was accepted as Iscon scope 1.38 for intense biotite alteration.